Published in final edited form as:
Wiley Interdiscip Rev Comput Mol Sci. 2016 ; 6(2): 86–110. doi:10.1002/wcms.1238.

The Virtual Multifrequency Spectrometer: a new paradigm for spectroscopy

Vincenzo Barone*
Scuola Normale Superiore, Piazza dei Cavalieri 7, 56126 Pisa, Italy

Abstract

On going developments of hardware and software are changing computational spectroscopy from a strongly specialized research area to a general tool in the inventory of most researchers. Increased interactions between experimentally-oriented users and theoretically-oriented developers of new methods and models would result in more robust, flexible and reliable tools and studies for the systems of increasing complexity, which are of current scientific and technological interest. This is the philosophy behind this review, which presents the development of a so-called virtual multi-frequency spectrometer (VMS) including state-of-the-art approaches in a user-friendly frame. The current status of the VMS tool will be illustrated by a number of case studies with special reference to infrared and UV-vis regions of the electro-magnetic spectrum including also chiral spectroscopies. Only the basic theoretical background will be provided avoiding explicit equations as far as possible, and pointing out the most recent advancements beyond the standard rigid-rotor harmonic-oscillator model coupled to vertical electronic excitation energies.

Keywords

anharmonic; vibronic; spectra line-shapes; virtual multifrequency spectrometer

1 Introduction

Spectroscopic techniques have become the methods of choice for analysing structural, dynamical, and environmental effects of molecular systems of increasing complexity in a very effective yet non-invasive way.1–5 Integrated approaches, in which different spectroscopic measurements are combined together to offer a comprehensive picture of complex systems and/or phenomena, are finding widespread use. However, the relationship between the spectroscopic outcome and the underlying physical-chemical properties is often indirect, and the disentanglement of the different factors playing a role in determining the overall result can be strongly facilitated by quantum mechanical (QM) computations, provided that the latter are able to couple reliability and feasibility.6 Small to medium-size semi-rigid systems in the gas-phase can be nowadays studied by QM methods with an accuracy rivalling that of the most sophisticated experimental techniques.7–12

*To whom correspondence should be addressed: vincenzo.barone@sns.it.

Europe PMC Funders Author Manuscripts

However, the situation is more involved for large, flexible systems of current technological and/or biological interest. In this connection, methods rooted into the density functional theory (DFT)13,14 and its time-dependent (TD-DFT)15,16 extension have revolutionised the field allowing effective computations of several properties with sufficient accuracy. When solvated systems are under study, an additional source of complexity arises, since the spectroscopic processes primarily induced by a well-localised chromophore are also significantly affected by the presence of more distant atoms, the “environment”. For this reason, many theoretical models have been developed in order to properly take into account the effect of the solvent molecules on the desired spectroscopic property17,18 especially in the framework of the polarisable continuum models (PCM).19

All those factors prompted my group to develop a virtual multifrequency spectrometer (VMS)20,21 providing user-friendly access to the latest developments of computational spectroscopy also to non-specialists. Together with the ongoing implementation of additional spectroscopies (i.e. electromagnetic field regions) in VMS, we have integrated a powerful graphical user interface (GUI),22 which can offer an invaluable aid in pre-organizing and presenting in a more direct way the information produced by in vitro and in silico experiments focusing attention on the underlying physical-chemical features without being concerned with technical details. We have thus at our disposal the VMS-Comp background,20,21 which takes care of QM computations of spectra and related high-performance computing (HPC) aspects and the VMS-Draw interface,22 which manages and simplifies direct interaction between users and data (see Figure 1). Both modules are either fully embedded (vibrational and electronic spectroscopy) or loosely bound (rotational and magnetic spectroscopy together with the GUI) to the GAUSSIAN package,23 which offers a large panel of utilities for dealing with stereo-electronic, dynamic, and environmental effects. At the same time, more general input-output facilities under development or ad hoc scripts permit effective interactions with other electronic structure codes (ESC’s),24–26 which give access to additional computational models (e.g. multi-reference wave function approaches) or properties (e.g. nonlinear parameters) not yet available in our reference QM suite. We are, of course, aware that several codes including additional electronic models, graphic engines, or simple command lines can be already interfaced to general purpose ESC’s. However, none of these tools offers all the characteristics we consider mandatory for state-of-the-art computational spectroscopy (e.g. anharmonic frequencies and intensities, vibronic contributions, etc.) and/or for a flexible user-friendly graphical tool including both general utilities needed by experimentally-oriented scientists (e.g.normalization, conversion, and other manipulations of several spectra at the same time) and advanced tools for theoreticians and developers (e.g. resonance raman (RR) spectra). In the following sections, after a summary of the general philosophy underlying the VMS project and of some technical aspects, we will perform a tour through the major spectroscopies illustrating, with the help of some case studies, the current status of VMS and the most important improvements planned for the near future. Particular attention will be devoted to a fully general formulation of anharmonic rovibrational and harmonic vibronic energies, which allows the simulation of complete spectral shapes for infrared (IR), vibrational circular dichroism (VCD), non-resonance and resonance Raman, and Raman optical activity (ROA

and RROA), electronic one-photon absorption and emission (OPA and OPE), electronic circular dichroism (ECD) and circularly polarized luminescence (CPL).

2 General background

As mentioned in the introduction, nowadays computational methodologies greatly facilitate the prediction of molecular properties along with their spectroscopic signatures, which in turn can be compared to the available experimental data.6 However, the standard analysis is often limited to the computational outcomes directly available from geometry optimisations followed by harmonic frequency computations. Analytic force constants and at least first derivatives of electric and magnetic properties are now available for a large number of quantum mechanical methods, in particular rooted into the density functional theory. So, equilibrium molecular structures and properties, relative energies of isomers and/or conformers, thermodynamic and kinetic properties as well as frequencies and infrared intensities in the framework of the rigid-rotor harmonic-oscillator (RRHO) model are usually provided directly by QM codes.

The information required for predicting and/or analyzing spectra in the field of vibrational spectroscopy are the vibrational frequencies and the corresponding intensities. Extension to other vibrational spectroscopies requires the availability of analytical (or numerical) first derivatives of other properties,6 which lead to routine simulations of harmonic IR, Raman and even VCD or ROA spectra in many quantum chemical packages. However, the harmonic oscillator approximation leads to a truncated description of the physical-chemical problem (e.g. vanishing intensities for overtones and combination bands). In fact, in order to fulfill the accuracy (for frequencies) and interpretability (for intensities) needs of experimentalists, it is mandatory to go beyond the so-called double-harmonic approximation accounting for both mechanical and electrical anharmonic effects.27

Coming to electronic transitions, absorption spectra are most often interpreted in terms of vertical excitation energies and related transition dipole moments, while simulation of emission spectra requires also optimisation of excited state geometries. The latter are nowadays rather routine even for large molecular systems mainly due to the advances within the TD-DFT theory, such as the development of effective analytic gradients28,29 and, very recently, of analytic Hessians,30,31 which are allowing a full characterization of excited electronic states. In this framework band-shapes are obtained by the convolution of vertical (or adiabatic) excitation energies by phenomenological (mostly symmetrical) distribution functions, completely neglecting the vibrational structure present in experimental spectra. Inclusion of vibronic effects is not only crucial for the interpretation of high-resolution data showing a detailed vibrational structure32,33 but also for low-resolution spectra, allowing to simulate realistic asymmetric band-shapes34 and to account correctly for the relative intensities of transitions.35,36

To go beyond the current state-of-the-art for analysis and prediction of spectra the ongoing efforts are mainly concentrated on the improvement of electronic QM models underlying computation of all molecular properties, including those related to spectroscopic observables. Taking advantage of the available developments within QM theory, my group

Europe PMC Funders Author Manuscripts

has taken another route, focusing attention on nuclear motion and environmental effects, which, although often overlooked, are mandatory for a meaningful comparison with experimental outcomes. In this framework, moving from the standard practice of extracting numerical data from experiment to be compared with QM results toward the direct comparison between recorded and computed spectra would strongly reduce any arbitrariness and allow a proper account of the information hidden behind both positions and shapes of spectral bands.20,27

The Virtual Multifrequency Spectrometer has been devised to overcome those limitations, with important efforts devoted to develop models able to account for anharmonic vibrational and harmonic vibronic effects and to implement them efficiently. VMS is especially effective for systems and phenomena localized in a limited space region, but possibly tuned by the more distant environment. To this end, several focused models are available, including different QM layers together with classical (possibly polarisable) atomistic environments and a polarisable continuum descritpion of bulk (solvent, nanoparticle, inert matrix, etc.) effects.37–39 Although this model (see Figure 2) has been extended also to fully dynamical treatments enforcing non-periodic boundary conditions (NPBC),40 in the present context we will refer explicitly only to time-independent or short-time limits of quantum dynamical approaches. Furthermore, proper treatment of non-equilibrium effects will be taken for granted without further explicit discussion.17,18,41 Finally, we will assume that the Born-Oppenheimer approximation7,42 is satisfied and that quantization of overall molecular rotations can be neglected, with the possible exception of Coriolis couplings.

In this framework, the physical-chemical properties of a molecular system can be described by separate potential energy surfaces (PESs) and by the corresponding property surfaces (PSs) for each electronic state together with the needed transition moments. Electronic, magnetic and mixed transitions between (ro-)vibrational energy levels of one or more potential energy surfaces give rise to a large number of spectroscopies, among which infrared, Raman as well as OPA and OPE electronic transitions along with their chiral counterparts (VCD, ROA, ECD and CPL). Vibrational averaging effects need to be taken into account also for other kinds of spectra (e.g. nuclear magnetic resonance (NMR) and electron spin resonance (ESR)). From a theoretical point of view all these different spectroscopies can be described within the same general framework sketched in Figure 3 starting from a single vibrational energy level in a specific electronic state and proceding towards transitions involving vibrational energy levels of multiple electronic states. We also define hybrid QM/QM’ schemes assuming that less expensive, yet reliable QM’ models are applied to the most involved computations, not feasible by higher-accuracy approaches, i.e. anharmonic corrections or definition of excited state PES. These are combined with refined values for the equilibrium structures and properties, harmonic force fields, or vertical excitation energies and transition moments.43

3 Selection of electronic quantum mechanical models

The basic reliability requirement of electronic QM models is related to the equilibrium structures, which are well defined as minima of the BO PES and exclude vibrational effects (present in experimental r_0, see Figure 3). In this context, the so-called semi-experimental

(SE) equilibrium geometry (r_e^{SE}),44,45 which is obtained by a least-square fit of experimental rotational constants of different isotopologues computationally corrected for vibrational contributions represents the most suitable reference for the validation of purely theoretical structures (r_e^{QM}). Recently, we have shown that r_e^{SE} accurate within 0.001 Å and 0.1 degrees for bond lengths and angles, respectively, can be obtained avoiding any refined post-Hartree-Fock (at least Coupled Cluster with Single Double and perturbative Triple excitations (CCSD(T))46 computation including complete basis set extrapolation (CBS)) by means of anharmonic vibrational corrections computed by global hybrid (GHF) or double-hybrid (DHF) functionals.47–50 This finding has led to the creation of an interactive database providing accurate geometries for a large number of small and medium-size molecules, along with practical recipes to derive highly accurate parameters for larger molecular systems.48,49 In this respect the choice of functional and basis set becomes crucial. Concerning the basis set, in general terms, polarized double-ζ basis sets augmented by difufse functions (e.g. 6-31+G(d,p), or SNSD27) are sufficient for GHFs,27,51–54 whereas more extended basis sets again including at least s and p diffuse functions for second-row atoms (e.g. aug-cc-pVTZ55 or maug-cc-pVTZ56) are mandatory for DHFs. 54,57 Improved accuracy can be obtained for specific properties by further extension of the basis set (e.g. additional core-valence functions for EPR58 or higher angular momentum diffuse functions for Raman spectroscopy27,52). Concerning next the choice of the functional, we have demonstrated for a set of small-to-medium sized molecular systems27,59 that some GHFs, in particular B3LYP and B97-1, provide very satisfactory results for vibrational anharmonic computations, with mean absolute errors with respect to experiment of about 10 cm^{-1}, whereas this is not the case for some of the most successful, but heavily parameterized last-generation functionals (M06-2X60 and ωB97X,61 for instance). Moreover, in view of studying larger systems where dispersion interactions might be important, a viable route is provided by Grimme's semi-empirical dispersion correction13 added to the B3LYP functional.62 Increased accuracy, even for relatively large systems, can be achieved with hybrid approaches where the harmonic part is computed at higher levels of theory (especially (CCSD(T)46 or double-hybrid B2PLYP14), and the anharmonic corrections are evaluated with much less computationally demanding (B3LYP) models27 (see Figure 4). Recent studies on IR spectra of pyruvic acid, allowed to further confirm the good accuracy of B3LYP anharmonic corrections63 and B2PLYP harmonic wavenumbers64 also for overtones and combination bands (see Table 1). The situation is more complex for chiroptical spectroscopies,6,65 which, in addition to the electric dipoles require, depending on the specific spectroscopy, also magnetic moments, frequency-dependent polarizabilities, frequency-dependent optical rotations, and frequency-dependent dipole-quadrupole tensors. Unfortunately, in most cases, reference high-level post-Hartree-Fock computations (i.e. at the CCSD(T) level with extended basis sets) are not yet feasible for these properties. In fact, only recently the first calculations of harmonic ROA spectra using coupled-cluster theory have been reported by Crawford and Ruud,66 including only single and double excitations (CCSD) in conjunction with a polarized double-ζ basis set. Furthermore, some spectra (like VCD and ROA) require not only the values, but also the relative orientations of the derivatives of electric and magnetic moments, which raises the problem of the so called mode robustness.67 Anyway, it has been shown that the effects due

to electron correlation are less pronounced than those originating from the truncation of the basis set52 and that standard GHFs (i.e. B3LYP) are more effective than MP2,68 actually performing remarkably well also in comparison with CCSD.66 To the best of our knowledge, little is known about the performances of recently developed functionals in the prediction of IR, Raman, VCD or ROA spectra, whereas, based on the results obtained to date, DHFs (e.g. B2PLYP) generally provide increased accuracy.27,54,57 Additionally, whenever long-range and/or dispersion effects need to be described, a viable solution is offered by long-range corrected functionals (e.g. CAM-B3LYP or B3LYP-D3). Concerning excited electronic states, the selection of the best functional and basis set is not easy and strongly depends on the problem under study,69–72 with larger differences related to the choice of the functional than to the basis set. In some cases (e.g. charge-transfer (CT) transitions) the TD-DFT/B3LYP computational model underestimates the transition energies, whereas its long-range corrected counterpart (CAM-B3LYP) improves the description of Rydberg and charge transfer states,73 and has been recently included in the set of the eight best performing density functionals72 for excited electronic state studies. Here again, much less is known about the performances of recently developed functionals with respect to chiroptical spectra (ECD, CPL), whereas significant improvements over TD-DFT/B3LYP in the prediction of Rotatory strengths is achieved by the TD-DFT/CAM-B3LYP computational model, which provides qualitatively correct results for a large interval of excited electronic states when employed in conjunction with basis sets of at least polarized double-ζ quality augmented by diffuse functions.74 The spectra simulations reported in the next sections have been performed taking into account all the above remarks about the selection of density functional / basis set. The remarkable agreement with experiments obtained in all cases, gives further support to the suggested recipes and strongly suggests that, even pending further developments, we already dispose of sufficiently reliable and robust tools for performing multi-spectroscopic simulations of molecules of current scientific and technologic interest in their natural environment.

4 Vibrational spectra

While the harmonic approximation can give satisfactory trends, it suffers from several limitations when a quantitative agreement is needed, for instance when highly resolved experimental spectra must be analyzed. Indeed, the harmonic transition energies are in most cases too high and the discrepancy with experiment increases with the number of quanta. Moreover, only fundamental bands will appear, since transitions to higher levels have systematically null intensities. In order to improve the model, it is necessary to account for the anharmonicity of the PES and to use an extended description of the property. Several approaches have been proposed to compute energies and transition moments at the anharmonic level, with different levels of achievable accuracy and computational cost.

One group of methods suitable also for large systems is based on vibrational self-consistentfield (VSCF)75–77 and its expansions including higher-order correlation effects. Here instead, we will discuss approaches based on the second order vibrational perturbation theory (VPT2),78,79 in particular, a general framework to compute thermodynamic properties, vibrational energies and transition intensities from the vibrational ground state to

fundamentals, overtones and combination bands,50,53,80–84 which can provide very good results at a reasonable computational cost.

4.1 General VPT2 framework for vibrational transition energies and intensities

Within the Born-Oppenheimer approximation,42 the molecular wavefunction Ψ can be separated into its electronic (ϕ) and nuclear (ψ) components.7 The nuclear wavefunction can be further factorized by assuming that the Eckart-Sayvetz conditions are met,85 since the translation ($|\psi^t\rangle$) part can be separated and the couplings between the vibrational (ψ^v) and rotational ($|\psi^r\rangle$) wavefunctions can be minimized,

$$|\Psi\rangle \approx |\phi\rangle|\psi^t\rangle|\psi^r\rangle|\psi^v\rangle$$

In the following only transitions between vibrational states are taken into account and the rotational dependence is neglected.

The theoretical background on which VPT2 relies and its practical use are described in more details in Refs.82,84 The presented analytical formulas, which are those implemented in VMS, are derived resorting to the Rayleigh-Schrödinger perturbation theory. In the literature, alternative approaches based on the canonical Van Vleck perturbation theory86 are also used to obtain VPT2 energies and intensities (see references87,88 for examples of such developments) along with approaches where the algorithm used to derive the formulas is implemented instead, so that the derivation is carried out each time a new calculation is needed.87

For vibrational energies, which are the eigenvalues of the vibrational Hamiltonian ($\hat{\mathcal{H}}$), energy terms beyond the harmonic approximation ($\hat{\mathcal{H}}^{(0)}$) are obtained by expanding the potential energy operator $\hat{V}$ of the anharmonic oscillator, in a Taylor series up to the fourth order:

$$\hat{\mathscr{H}}^{(1)} = \frac{1}{6}\sum_{i=1}^{N}\sum_{j=1}^{N}\sum_{k=1}^{N}\frac{\partial^3\hat{V}}{\partial q_i \partial q_j \partial q_k} q_i q_j q_k \quad (1)$$

$$\hat{\mathscr{H}}^{(2)} = \frac{1}{24}\sum_{i=1}^{N}\sum_{j=1}^{N}\sum_{k=1}^{N}\sum_{l=1}^{N}\frac{\partial^4\hat{V}}{\partial q_i \partial q_j \partial q_k \partial q_l} q_i q_j q_k q_l \quad (2)$$

where the third and fourth derivatives of the potential energy V (in cm^{-1}) with respect to the dimensionless normal coordinates $\boldsymbol{q}$, are also called cubic and quartic force constants (k_{ijk} and k_{ijkl} respectively). By developing the vibro-rotational contribution term in the nuclear Hamiltonian in a Taylor series, an additional element appears in $\hat{\mathcal{H}}^{(2)}$ related to the so-called Coriolis couplings.

The vibrational energies of linear, symmetric and asymmetric tops can be expressed for both minima and first-order saddle points as

$$\varepsilon_{\mathbf{n},\mathbf{l}}=\varepsilon_0+\sum_i \hbar\sqrt{\lambda_i}n_i+\sum_i\sum_{j\geq i}\delta_{ij}^F\chi_{ij}\left[n_in_j+n_i\frac{d_j}{2}+n_j\frac{d_i}{2}\right]+\sum_s\sum_{t\geq s}g_{st}I_sI_t \quad (3)$$

with,

$$\delta_{ij}^F=(1-\delta_{iF})(1-\delta_{jF})+\delta_{iF}\delta_{jF} \quad (4)$$

where $\lambda_i=\omega_i^2$ (frequency of vibrations), the transition vector (i.e., the normal mode with the non-degenerate imaginary frequency) is labeled by the subscript F, δ_{ij} is the Kronecker's delta, **n** and **l** are respectively the principal and angular vibrational quantum numbers, and d_i is the degeneracy of mode *i*; with the the subscripts *i* and *j* used to indicate generic vibrational modes, degenerate or not, whereas *s* and *t* refer to the degenerate modes only.

It is remarkable that the zero point energy ε_0 can be written in a resonance-free way in terms of harmonic frequencies together with cubic and semi-diagonal quartic force constants. The same anharmonic force constants enter the $\boldsymbol{\chi}$ matrix, which contains, however, potentially resonant terms (see next section).84

Since electric and magnetic dipoles, together with polarizability tensors, are functions of the normal coordinates, general equations for the intensities of different spectroscopies can be derived by making reference to a generic property ***P*** expanded in a Taylor series about the equilibrium geometry up to the third order.

In order to lift at least part of the overall complexity of the VPT2 expansion for properties,some simplifications have been proposed, for instance by considering only one type of anharmonicity, either the electric one (only ***P*** is expanded) or the mechanical one (development of ψ^v).89–91 The first approximation involves only a few terms and is sufficient to get non-vanishing intensities for transitions between states differing by up to 3 quanta. Full derivations including both terms, however, are error-prone and the first correct formulas were proposed by Handy and coworkers, who derived full equations for fundamentals, combination bands and overtones up to 2 quanta.92 Stanton and Vàzquez later proposed equivalent, albeit more compact formulas using the Rayleigh-Schrödinger perturbation theory93,94 but limited to the transitions originating from the vibrational ground state. As those transitions are generally predominant (excited initial states have a lower population with respect to the ground state) we have followed the same route. Generalization to any initial state can be achieved in several ways, either by obtaining at runtime the required formulas for the state of interest, or by deriving once for all the equations for an arbitrary initial state $|\boldsymbol{v}\rangle$ and implementing the corresponding formulas. A general formula, which covers IR, Raman, VCD and ROA spectroscopies as particular cases82 has been derived and implemented in the VMS-Comp module.

It is rather straightforward to obtain anharmonic intensities for one- and two-quanta transitions, the latter corresponding to first overtones ($|\mathbf{0}\rangle \rightarrow |2_i\rangle$) and two-states combination bands with each mode excited by one quantum ($|\mathbf{0}\rangle \rightarrow |1_i 1_j\rangle$). If a wider region of the spectrum is desired, for instance including a significant part of the near-infrared (NIR) region, transitions to higher states may be of interest. Like for two quanta, transition moments for three-quanta transitions, which correspond to second overtones ($|\mathbf{0}\rangle \rightarrow |3_i\rangle$) and combination bands ($|\mathbf{0}\rangle \rightarrow |2_i 1_j\rangle$ and $|\mathbf{0}\rangle \rightarrow |1_i 1_j 1_k\rangle$) can be gathered in a single formula.83 To go beyond three quanta transitions, higher orders of the Taylor expansion of the property and Hamiltonian operators would be needed, that is up to the fourth (VPT4) or sixth (VPT6) order of the vibrational perturbation theory.

Equations for the transition energies84 and transition moments82,83 allow to obtain fully anharmonic IR, Raman, VCD and ROA spectra at the VPT2 level.

4.2 Resonances in VPT2 calculations

Another practical issue in the calculation of anharmonic energies and intensities is the presence of resonances. The most critical ones for the energies are the so-called Fermi resonances, of type I ($\omega_i \approx 2\omega_j$) and type II ($\omega_i \approx \omega_j + \omega_k$), which may result in unphysical anharmonic corrections, due to vanishing or nearly vanishing denominators of some terms in the χ matrix entering equations for vibrational energies (Eq. 3). Since these contributions are related to the first-order perturbative Hamiltonian, they are classified as first-order resonances, and are often referred to as 1-2 resonances. A correction needs to be applied in order to get reliable values, and several strategies have been explored and proposed in the literature.50,53,87,95 A robust control procedure combines the simplest strategy of setting a threshold and comparing the absolute values of the wavenumber difference "$\omega_i - (\omega_j + \omega_k)$" (or "$\omega_i - 2\omega_j$" for the special case $k = j$), which is a first step, followed by another one only if there is a risk of resonance, that is if the frequency difference is small enough. The second step, uses the test proposed by Martin and coworkers,95 comparing VPT2 terms with their two-state variational equivalent. It is thus possible to assess the deviation of a given VPT2 term from a suitable estimate of its variational counterpart. If the deviation becomes too high, the term is considered resonant.

The identification and removal of resonant terms, however, result in a truncated VPT2 treatment. In order to get better results, the common strategy is to perform in a successive step a variational treatment, using the VPT2 energies as diagonal elements of the variational matrix and the missing terms as off-diagonal elements. The complete procedure (removal of resonant terms followed by variational treatment) has been called GVPT2 (generalized VPT2) or VPT2+K (also VPT2+WK) by different authors.50,88,96 All those methods rely on the initial definition of the resonant terms, which has an empirical part in the definition of the thresholds. In order to avoid this step, an alternative method has been proposed where all potentially resonant terms are replaced by non-resonant variants. As a full variational treatment of so many terms would become prohibitive for large molecules, the missing terms are individually replaced by a model variational form. This approach has been called degeneracy-corrected PT2 (DCPT2) by its authors and does not use any threshold.97 However, it relies on a simplified model for the transformation, which only holds under

some specific conditions. As a result, it can lead to significant discrepancies with respect to the correct VPT2 treatment, in particular far from resonance. This error can be considerably reduced by introducing a transition function which uses the standard VPT2 formulation far from resonance and the DCPT2 alternative otherwise, leading to the so-called hybrid DCPT2-VPT2 (HDCPT2) model.53

The procedures to identify resonances in the vibrational energies, and the subsequent corrections have been already well tested and have proven to be able to deliver accurate results in conjunction with several QM models27 (see also Figure 4 and Table 1).

The problem of Fermi resonances is also present for intensities with the same risk of an incorrect account of the anharmonic correction. A common solution is to use the list of terms identified as resonant from the vibrational energy calculations, the eigenvalues of the Hamiltonian, and remove occurrences of those terms in equations for transition moments. Then, the eigenvectors (L_E) obtained from the diagionalization of the variational matrix used for the vibrational energies are employed to correct the transition moments as,

$$\langle \boldsymbol{P} \rangle_{if[1]}^{\mathrm{new}} = L_E \langle \boldsymbol{P} \rangle_{if[1]}^{\mathrm{VPT2}}$$

Another kind of resonances, sometimes omitted since they do not directly lead to potentially strong numerical inconsistencies like Fermi resonances, are the Darling-Dennison resonances. Contrary to Fermi resonances, they are of second order (they are related to $\hat{\mathcal{H}}^{(2)}$) and do not affect the calculation of the $\boldsymbol{\chi}$ matrix. Indeed, they are included successively in the full variational matrix as off-diagonal elements, where the diagonal elements are the VPT2 energies. By extension, 1-1 ($\langle \boldsymbol{v} + 1_i | \hat{\mathcal{H}} | \boldsymbol{v} + 1_j \rangle$) and 1-3 ($\langle \boldsymbol{v} + 1_i | \hat{\mathcal{H}} | \boldsymbol{v} + 1_j + 1_k + 1_l \rangle$) resonances are sometimes referred to as Darling-Dennison and a complete treatment of those cases has been proposed by Martin and Taylor,98 recently rederived and corrected by Rosnick and Polik.88

Also in this case, a critical step is represented by proper handling of resonance tresholds. However, since their impact is not so directly visible, and due to the still rather scarce studies including anharmonic intensities, less investigations have been carried out on the definition of robust procedures to perform automatically and efficiently this task. While already important for energies, 1-1 and 1-3 resonances become critical in the case of intensities, respectively for the cases of fundamental bands and three-quanta transitions. Indeed, the presence in denominators of "$\omega_i - \omega_j$" in the first case and "$\omega_i - (\omega_j + \omega_k + \omega_l)$" in the second one may result in excessive anharmonic contributions, so the resonant terms must be properly identified and corrected. Robust schemes for those types of resonances, are being worked out, however some promising procedures to solve this issue have been already proposed.82,96

4.3 Simulation of anharmonic spectra

The main requirement to carry out anharmonic calculations is the availability of energy and property derivatives at equilibrium geometries. While some methodologies have been proposed to compute those quantities analytically,99–102 this remains mostly done

nowadays by means of numerical differentiations of the potential energy ***V*** and properties ***P*** with respect to the to the mass-weighted normal coordinates. That procedure allows effective anharmonic computations for all QM models for which at least the second derivatives of the energy and the first derivatives of the properties can be computed analytically, giving access to all cubic and quartic force constants with at most three different indices (up to k_{iijk}) and property derivatives with at most two different indices. Of course, the step used in the differentiation (δQ_i) must be small enough to correctly compute the derivatives, but large enough to ensure numerical stability.

For purposes of illustration, Figure 5 compares different models to simulate vibrational spectra taking the experimental gas-phase IR spectrum of napthalene as reference.83 It is clear that within the harmonic approximation all bands are shifted and many transitions are missing, while applying uniform scaling factor improves the band positions but will always produce the same pattern as the harmonic spectrum. Once energies are corrected by VPT2 computations the positions of fundamental bands agree well with experiment, but several transitions are still missing. Finally, the full anharmonic computation, accounting for both mechanical and electrical anharmonicities, leads to very good agreement with experiment for both band positions and intensities, including spectral ranges fully due to the non-fundamental transitions, i.e the 1500-2000 cm^{-1} range shown in Figure 5 or the NIR region. 83

Figure 6 reports IR, Raman, VCD and ROA spectra of methyloxirane, as compared with experimental results.103,104 For infrared spectra, a very good agreement with experiment, for both band positions and IR intensities, has been obtained by coupling the harmonic Coupled Cluster (CC) contributions with anharmonic effects computed at the B3LYP level. 104 The same highly accurate CC/B3LYP force field is applied here in conjunction with the B3LYP-based property surfaces to simulate Raman, VCD and ROA spectra, demonstrating how several spectroscopic techniques can be combined together to get a more complete and accurate picture of vibrational properties, with full support of computational studies within the VMS tool. As a last point, let us underline again that the reliability of different bands in the computed VCD and ROA spectra should be always checked by using one of the robustness criteria suggested for harmonic computations.105,106 All of them will be shortly included in VMS also at the anharmonic level, starting from IR and VCD (respectively Raman and ROA) intensities thanks to proper generalizations of electric and magnetic moments.

5 Vibronic spectra

5.1 General TI-TD vibronic framework

As already mentioned in the introduction, inclusion of vibro-electronic couplings is critical to simulate correctly both high-resolution electronic spectra, where single vibronic bands can be detected, and low-resolution spectra, where the convolution of all the vibronic bands may lead to asymmetric bandshapes. From a theoretical point of view, the presence of two different electronic states introduces additional difficulties, and therefore further approximations must be invoked. Here, in addition to the approximations presented above (Born-Oppenheimer approximation, Eckart conditions), the harmonic model will be used to

describe the molecular vibrations except for possible corrections of vibrational frequencies by estimates based on VPT2 results for the ground electronic states and simple linear models (vide infra). Within this framework, we have derived the following general expression for the vibronic contributions to the transition between electronic states A and B, supporting several spectroscopies, namely one-photon absorption (OPA) and emission (OPE), as well as electronic circular dichroism (ECD) and circularly polarized luminescence (CPL),

$$I=\alpha\omega^{\beta}\sum_{m}\sum_{n}\rho_{\gamma}\boldsymbol{d}^{\mathrm{A}}_{mn}\boldsymbol{d}^{\mathrm{B}}_{mn}*\delta\left(\frac{E_n-E_m}{\hbar}-\omega\right) \quad (5)$$

where I is a general experimental observable, ω is the incident frequency, m and n are the lower and higher vibrational states of the transition, E_m and E_n are their respective energies and $\boldsymbol{d}^{\mathrm{A}}_{mn}$ and $\boldsymbol{d}^{\mathrm{B}}_{mn}$ are electronic transition dipole moments between them (which can be either electric or magnetic, depending on the type of spectroscopy). The definition of I, $\boldsymbol{d}^{\mathrm{A}}_{mn}$, $\boldsymbol{d}^{\mathrm{B}}_{mn}$, γ, α and β changes with the type of spectroscopy, which is used. A more detailed discussion can be found in refs.21,74,107

In practice, additional approximations must be introduced to use equation 5. First of all, since analytical expressions for the electronic transition moments are not known, a Taylor series with respect to the mass-weighted cartesian normal coordinates **Q** about the equilibrium geometry of one of the electronic state is usually employed,

$$\boldsymbol{d}^{\mathrm{X}}_{mn}(\mathbf{Q})=d^{\mathrm{X}}_{mn}(\mathbf{Q}_{\mathrm{eq}})+\sum_{i=1}^{N}\left(\frac{\partial\boldsymbol{d}^{\mathrm{X}}_{mn}}{\partial Q_i}\right)_{\mathrm{eq}}\mathbf{Q}_i+\circ\ (\mathbf{Q}) \quad (6)$$

where X can be either A or B. In equation 6, the expansion is usually limited to the first two terms, where the zeroth-order term corresponds to the well-known Franck-Condon approximation,108,109 while the first-order corrections are usually referred to as Herzberg-Teller terms.110 Finally, the linear transformation proposed by Duschinsky111 can be used to relate the cartesian normal coordinates of the two electronic states,

$$\overline{\mathbf{Q}}=\mathbf{J}\overline{\overline{\mathbf{Q}}}+\mathbf{K} \quad (7)$$

where $\bar{\mathbf{Q}}$ and $\bar{\bar{\mathbf{Q}}}$ are the normal coordinates of the initial and final states, respectively. **J** is the Duschinsky matrix and **K** is the shift vector. It is noteworthy that equation 7 is well-suited for semi-rigid systems, but may be inaccurate for the description of molecules undergoing large-amplitude deformations upon electronic excitation. Furhermore, the definition of **J** and **K** changes with the harmonic model used for the final state PES. Due to the limitations of the harmonic approximation, two different representations are usually employed. In the first one, referred to as adiabatic, the PES of the final state is expanded about its own equilibrium geometry (Adiabatic Hessian, AH), while in the vertical approximation it is expanded about the equilibrium geometry of the initial state (Vertical Hessian, VH). In both cases, simplified

Europe PMC Funders Author Manuscripts

models, where mode-mixing as well as frequency change effects are neglected, can be derived (Adiabatic Shift, AS and Vertical Gradient, VG, respectively).74,112

By using those approximations, the sum given in equation 5 can be expressed in terms of overlap integrals between the vibrational levels of the two electronic states, usually referred to as Franck-Condon integrals. In the so-called time-independent (TI) approach, those integrals are calculated using either analytical or recursive formulae. The second approach is better-suited for a general implementation and is actually used in the VMS tool.74,112 The main limitation of this model relies on the number of Franck-Condon integrals to compute, which increases significantly with the size of the target system. In order to make computations feasible also for medium- and large-size systems, prescreening strategies can be profitably employed, to select *a-priori* the Franck-Condon integrals, giving the largest contributions to the final spectrum. In our implementation, a class-based prescreening system is employed,113 which has been shown to perform a good job also for large-size semi-rigid systems. Anyway, the computational costs of the TI procedure increases considerably when temperature effects are included, since in this case several initial states must be considered,114 and this computational procedure may become prohibitive also for medium-size systems. In order to overcome those limitations, the parallel time-dependent (TD) framework can be employed, where the vibronic spectrum is calculated from the Fourier transform of the autocorrelation function, as follows:

$$\begin{aligned} I &= \alpha' \omega^{\beta} \int_{-\infty}^{+\infty} dt\, \mathbf{Tr}\left(\boldsymbol{d}_e^{\mathrm{A}}\, e^{-\bar{\bar{\tau}}\bar{\bar{H}}}\, \boldsymbol{d}_e^{\mathrm{B}*}\, e^{-\bar{\tau}\bar{H}} \right) e^{i(\omega_{\mathrm{ad}}-\omega)t} \\ &= \alpha' \omega^{\beta} \int_{-\infty}^{+\infty} dt\, \chi(t) e^{i(\omega_{\mathrm{ad}}-\omega)t} \end{aligned} \tag{8}$$

where $\bar{H}$ and $\bar{\bar{H}}$ are the vibrational Hamiltonian operators of the lower and upper states, $\bar{\tau}$ and $\bar{\bar{\tau}}$ are complex variables, depending on the time t and the temperature T and ω_{ad} is the adiabatic energy separation between the two states. $\chi(t)$ is the transition dipole moment autocorrelation function, which has an analytical (albeit complicated) expression within the approximations out-lineded above.107,115,116 Therefore, equation 8 can be used to calculate the vibronic spectrum by carrying out the Fourier integral using a numerical integration algorithm. Let us remark that in the TD formulation (at variance with the TI one) infinite summations are no longer present. As a consequence, there is no need of using prescreening strategies and the computational cost of the overall procedure is independent on the temperature. Moreover, both the TI and the TD formulation can be extended, at the same level of approximation, to the calculation of resonance Raman (RR)41,117,118 and resonance Raman optical activity (RROA)119 spectra. Implementation of complementary TD and TI approaches within VMS permits to take advantage of their respective strengths: the TD route is characterized by the automatic inclusion of all vibrational states and, possibly, temperature effects, providing band-shapes, while the TI route permits to identify and assign individual vibronic transitions.

5.2 Simulation of vibronic spectra

The simulation of vibrationally resolved electronic spectra represents an invaluable aid for the interpretation of well resolved experimental data in the gas phase,33,43 allowing to

analyze in detail and assign all vibronic transitions (see Figure 7). It should be noted that the present single-state approach does not allow yet to take into account all possible effects (such as non-adiabatic couplings) influencing the spectral outcome. Nevertheless, it has been able to simulate qualitatively correct spectral line-shapes even when experimental data encompass large energy intervals and several excited electronic states (see Figure 7), especially if possible TD-DFT inaccuracies in the prediction of absolute VE's are corrected by more accurate post-Hartree-Fock computations within hybrid QM/QM' approaches.

However, vibronic effects are equally important also for the analysis of less-resolved electronic spectra, like those recorded in solution. In that case proper account of the underlying (even if not directly visible) vibrational structure allows to correctly predict relative band intensities. As an example, some of the electronic transitions entering the UV-Vis spectrum of alizarin (see Figure 8) show similar oscillator strengths, so that in the spectra simulated at the basic VE level these bands would be broad or narrow, respectively, depending on the value (large or small) of the half-width at half-maximum (HWHM). On the contrary, when taking into account the vibronic structure, two transitions show very different band-shapes, a broad $S_1 \leftarrow S_0$ band and a narrow $S_6 \leftarrow S_0$ band, in agreement with the experimental findings.36 These effects can be even more important for chiral spectroscopies, as demonstrated, for instance, by the ECD spectrum of dimethyloxirane, whose overall line-shape is determined by a cancelation of positive and negative vibronic transitions from close-lying electronic states,21,120 or even within the same electronic transition due to the Herzberg-Teller effects.20,21

For purposes of illustration, a detailed analysis of different effects underlying the final experimentally observed band shape is presented for the case of UV-vis spectra of chlorophyll-*a*.34 The spectrum line-shape is dominated by the contributions from transitions to the S_1, S_3 and S_4 excited electronic states, with non-negligible contributions from transitions to S_2, giving rise to the Q_y, B_y, B_x and Q_x bands respectively, as shown in Figure 9. An excellent agreement between the simulated and experimental electronic spectra in the entire UV-vis range is obtained only after inclusion of all the relevant contributions, namely (*i*) bulk solvent effects by means of the PCM; (*ii*) vibronic structure of the chlorophyll moiety, and (*iii*) contributions from the intra-molecular vibrations by considering explicit solvent molecules (within possible penta- and hexa-coordinations) (see Figure 10 and Ref. 34 for details).

6 Toward larger and flexible molecular systems

6.1 Reduced dimensionality models

For larger systems (say above 30 atoms) the main computational burden is related to the derivation of the anharmonic PES and PS by numerical differentiation of analytical energy and property derivatives along the normal modes, which increases steeply with the systems size. Indeed for a N-atomic non-linear system derivation of full-dimensionality semi-diagonal quartic PES requires 6N-11 Hessian computations, becoming also individually more expensive as N increases. However, for larger systems it is also often true that only some vibrations are of an interest, for instance the most intense bands or selected/measured spectral ranges. In such cases the computational cost can be significantly scaled down by

reduced-dimensionality (RD) computations,121 for which the numerical differentiation of analytical Hessian is performed only along some selected normal modes (active modes, *a*). Those RD force-fields include all k_{ajk} and k_{aajk} force constants with at least one and two active modes, respectively (the subscripts *j* and *k* indicate generic vibrational modes, active or not). Thus, the corresponding RD-VPT2 computations take into account all essential anharmonic constants for active modes, along with the couplings with the other modes which, instead, are treated at the harmonic level. In this sense, the RD approach is very different from the simple few-mode models, which often take into account only diagonal anharmonicity (D) or couplings only within a reduced set of normal modes (C).

A remarkable example showing the effectiveness of the RD model is offered by time-resolved infrared spectroscopy (TRIR) studies of photoinduced processes in metal-carbonyl-diimine complexes.122 Electronic and structural changes in these systems can be effectively monitored by the changes in band positions and intensities of carbonyl stretching vibrations ν(C=O), which show very strong, isolated IR bands around 2000 cm^{-1}. For $Re(Cl)(CO)_3(\alpha$-diimine) complexes ((α-diimine= 2,2'-bipyridine (**Rebpy**) or pyridylimidazo[1,5-*a*]pyridine (**ReGV**) it is natural to consider all the three CO stretchings in a three-mode (RD3) computations. In such case only 7 Hessian computations are required for both systems, so they were only 7 times more expensive than the simplest harmonic approach, to be compared with factors of 157 and 289 for the full dimensionality case of **Rebpy** and **ReGV**, respectively. Such computations are sufficient to generate all terms necessary for the accurate anharmonic description of the ν(C=O) vibrations of interest. For Rebpy the RD3 model leads to about 10,000 non-zero k_{ajk} and k_{aajk} terms, while simple models based on 3 modes includes only 6 (diagonal, D3) and 16 (coupled, C3) unique force constants, respectively.

Comparison with experiment shows a very good agrement for both full (FD) and RD3 anharmonic computations (see Figure 11 and Table 2), which in turn agree with each other within 3 cm^{-1}, for both the ground and excited electronic states. Much larger average differences with respect to FD are obtained with over-simplified models including only the three ν(CO) stretches (about 11 cm^{-1} and 36 cm^{-1}, for C3 and D3 model, respectively).

The RD3 scheme based on the C=O stretching spectral range provided also improved agreement with experiment for chlorophyll-*a* in tetrahydrofuran solution.20,121 Other cases particularly suitable for RD computations include hybrid organic-inorganic systems like e.g. glycine adsorbed on a silicon cluster,123 where even taking into account all normal modes of the adsorbate the computational cost remains substantially lower than for the total system. It can be noted that RD schemes can also be very useful whenever more extended parts of the spectra, or delocalized phenomena (hence also larger fraction of normal modes) need to be considered (see Resonance Raman spectra of chlorophyll-*a*41 or $[Ru(bpy)_3]^{2+}$ 118) still leading to significant savings of computer time while providing remarkablyy accurate results.

6.2 Beyond semi-rigid molecules: harmonic models in internal coordinates

As outlined above, reduced-dimensionality schemes are particularly appealing to extend the range of application of anharmonic models to large-size systems. However, the reliability of

those schemes depends heavily on the coordinate system, which is used in the simulation. In particular, a coordinate system giving a nearly-diagonal representation of the PES allows to safely replace the full-dimensionality problem by several, lower-dimensionality problems, which can be treated separately.

Even if for rigid systems use of the standard cartesian coordinates is sufficient to satisfy the requirements outlined above, for large and flexible systems the choice of the coordinates used in the simulation is more relevant. In fact, in presence of large-amplitude modes (such as torsions, out-of-plane modes or ring deformations), curvilinear internal coordinates provide a much more diagonal representation of the potential energy surface with respect to their cartesian counterparts. However, cartesian coordinates have the advantage of being defined univocally, whereas, starting from the same molecular topology, several non-equivalent sets of non redundant internal coordinates can be built. In order to automatize as much as possible the overall computational procedure, a first step is to define a fully-automatized protocol to build a non-redundant set of internal coordinates to study molecular vibrations at the harmonic level.124 Within this protocol, the so-called delocalized internal coordinates (DICs),125 which are commonly used in geometry optimizations and can be generated straightforwardly starting from the molecular topology, are used as the non-redundant set of coordinates. Up to now, this approach has been applied to the simulation of vibronic spectra at the harmonic level, since already at this level significant improvements in the theoretical results are possible. One limit of DICs is that they often correspond to linear combinations of internal coordinates of different types and possibly localized in different spatial regions. Several methods have been proposed to avoid these unwanted mixings. Among them, the so-called weighted internal coordinates126 are already available in VMS, whereas inclusion of the more refined and chemically sound natural internal coordinates proposed long time ago by Pulay and coworkers127 requires significant programming effort and is still under development. It is worth mentioning that the theoretical framework presented in the previous section for the simulation of vibronic spectra can be modified to support also internal coordinates, simply by changing the definition of the Duschinsky transformation. As an example, in the upper panel of Figure 12, the theoretical OPA spectrum of imidazole in water for the $S_2 \leftarrow S_0$ electronic transition is reported. It is noteworthy that, even if the single vibronic peaks cannot be detected, the overall vibronic broadening is significantly larger using cartesian coordinates than internal ones, and the absolute intensity is lower by one order of magnitude. In fact, using cartesian coordinates, the modes of the two electronic states are significantly coupled (the deviations of **J** from a diagonal matrix are significant) with respect to the internal coordinate case. Therefore, a larger number of vibronic transitions are active, leading to an excessive broadening of the final spectrum and to lower FC factors. The impact of the coordinate systems is relevant also in the simulation of the resonance Raman spectrum of imidazole in water (which is reported in the lower panel of figure 12), where the relative intensity of the peaks depends strongly on the choice of the coordinate system.

Let us recall that the further inclusion of anharmonic effects within this internal-coordinate framework is far from being straightforward. However, as already remarked above, using internal coordinates, the overall set of normal modes can be divided into several subsets of

nearly-indepdendent modes. Therefore, it is possible to derive hybrid schemes, where coordinates belonging to different sets are treated at different levels of approximation (harmonic models, VPT2 route or more accurate anharmonic models), therefore allowing the efficient inclusion of anharmonic effects also for larger size systems. The definition of those models is currently under study in our group, and an example is provided in Figure 13 by a variational treatment of the large amplitude (torsional) motion of methanol.

7 Magnetic Spectroscopies

As mentioned in the introduction, the focus of this contribution is on vibrational and vibronic spectra, but the virtual multifrequency spectroscopy can also deal with magnetic spectroscopies, where the concept of effective Hamiltonian (here spin Hamiltonian) is again central to the discussion of and analysis of the results. From the point of view of computational spectroscopy, the spin Hamiltonian is first of all decomposed into a set of individual operators corresponding to specific physical effects. Once suitable theoretical/computational descriptions are established for these operators a viable link is obtained between computed and observed spectral parameters. In the case of NMR spectroscopy, a general formulation of the spin Hamiltonian is the following:6

$$\hat{H}_s(\mathrm{NMR}) = -\sum_{C=1}^{N} \hbar\gamma_C \mathbf{B}\cdot(1-\sigma_C)\cdot\mathbf{I_C} + \frac{\hbar^2}{2}\sum_{C=1}^{N}\sum_{D=1,D\neq C}^{N} \gamma_C\gamma_D \mathbf{I_C}\cdot(\mathbf{D_{CD}}+\mathbf{K_{CD}})\cdot\hat{I}_D \quad (9)$$

Where γ_C are nuclear magnetogyric ratios; $\mathbf{I_C}$ nuclear spin operators (related to the nuclear magnetic dipole moments, $\mu_\mathbf{C} = \hbar\gamma_C\mathbf{I_C}$); $\sigma_{C\leftrightarrow}$ magnetic shielding tensors (accounting for the shielding effect of the electrons); $\mathbf{D_{CD}}$ dipolar coupling tensors (which describe the direct couplings of the nuclear magnetic dipole moments); and $\mathbf{K_{CD}}$ reduced indirect nuclear spin-spin coupling tensors (which describe the indirect couplings of the nuclear dipoles caused by the surrounding electrons). Other terms can be needed for specific situations, like, e.g. paramagnetic systems or molecules containing quadrupolar nuclei.

Analogously a suitable spin Hamiltonian for building ESR spectra of free radicals $\hat{H}_s$ can be defined as:6

$$\hat{H}_s(\mathrm{EPR}) = \mu_\mathrm{B}\mathbf{S}\cdot\mathrm{g}\cdot\mathbf{B} + \frac{1}{\hbar\gamma_I}\mathbf{S}\cdot\mathbf{A}\cdot\mu_\mathbf{I}\,, \quad (10)$$

where the first term is the Zeeman interaction between the electron spin and the external magnetic field in terms of the Bohr magneton, $\mu_\mathrm{B}=e\hbar/2m_ec$, and the electronic g-tensor. The second term is the hyperfine interaction between **S** and the nuclear spin **I**, described through the hyperfine coupling tensor **A**. Also in this case, additional terms can be needed for more general situations (e.g. more than one unpaired electron).

Then, the first step is to compute reliable structural parameters and all the magnetic tensors entering the equations above, possibly including average interactions with the environment

Europe PMC Funders Author Manuscripts

(by discrete-continuum models), and short-time vibrational averaging effects. Next, the calculated molecular parameters are fed into dynamical models based on classical molecular dynamics, coarse-grained dynamics or, above all, stochastic modeling.6 Our approach is based on the solution of the Stochastic Liouville quation (SLE),128 which is essentially a semiclassical model based on the Liouville equation for the magnetic probability density of the molecule augmented by a stochastic operator,129 which describes the relevant relaxation processes that occur in the system and is responsible for the broadening of spectral lines. In the case of ESR spectra of nitroxide radicals and polyradicals, magnetic tensors computed by global hybrid density funcionals in conjunction with purposely taylored basis sets and the polarizable continuum model plus a limited number of molecules belonging to the cybotactic region (only for hydrogen bonding solvents) define a general and robust procedure, which allows the quantitative reproduction of experimental spectra without any adjustable parameter. The computer code developed to this end (ESPIRES)130 is included in the latest version of VMS. An example of the nitroxide spectrum is shown in Figure 14. The implementation of an analogous fully automated code for NMR spectroscopy is in progress, but a first version for the simulation of 1D and 2D NMR solid state spectra is already operative, and is interfaced with several molecular and solid-state codes. As an example, Figure 14 shows the ^{17}O NMR spectrum of benzoic acid dimer.

8 Conclusions

Spectroscopic quantities can be evaluated from fully quantum mechanical approaches able to provide equilibrium geometries and properties together with their derivatives with respect to geometric and field (electric and magnetic components) variables. The availability of most of these quantities in several electronic structure codes at different levels of sophistication has paved the route toward the development, validation and general use of models going beyond the standard harmonic-oscillator / rigid rotor approximation for vibrational spectroscopies and beyond the vertical transition energy model for electronic spectroscopies. Moreover, the development of a purposely taylored graphical user interface is allowing an effective and user-friendly analysis of the huge amount of results produced by these models and a direct vis-à-vis comparison between simulated and experimental spectra for complex molecular systems in their natural environment. This new situation and its perspectives have been shortly reviewed in this contribution also by means of case studies with the aim of introducing a new paradigm in the accurate and user-friendly simulation of various kinds of spectra for molecules of current interest in several fields of research and technology.

Acknowledgments

The research leading to these results has received funding from the European Union's Seventh Framework Programme (FP7/2007-2013) under the grant agreement N^{o} ERC-2012-AdG-320951-DREAMS. All the present and past members of the DREAMS center (http://dreams.sns.it) are acknowledged for their contributions to the ongoing development of the VMS tool with special thanks to Alberto Baiardi, Malgorzata Biczysko (now at Shanghai University) and Julien Bloino (now at ICCOM-CNR, Pisa UOS).

References

(1). Laane, J., editor. Frontiers of Molecular Spectroscopy. Elsevier B.V.; 2008. p. 740

(2). Berova, N.Polavarapu, PL.Nakanishi, K., Woody, RW., editors. Comprehensive Chiroptical Spectroscopy: Instrumentation, Methodologies, and Theoretical Simulations. John Wiley & Sons, Inc; Hoboken: New Jersey: 2012.

(3). Magyarfalvi G, Tarczay G, Vass E. Vibrational circular dichroism. WIREs Comput Mol Sci. 2011; 1:403–425.

(4). Alonso, JL., López, JC. Topics in Current Chemistry. Springer; Berlin Heidelberg: 2015. Microwave Spectroscopy of Biomolecular Building Blocks; p. 1-67.

(5). Rijs, AM., Oomens, J., editors. Topics in Current Chemistry. Vol. 364. Gas-Phase IR Spectroscopy and Structure of Biological Molecules. Springer International Publishing; 2015.

(6). Barone, V., editor. Computational Strategies for Spectroscopy, from Small Molecules to Nano Systems. John Wiley & Sons, Inc; Hoboken: New Jersey: 2011.

(7). Jensen, P., Bunker, PR. Computational Molecular Spectroscopy. John Wiley and Sons, Ltd; Chichester, UK: 2000.

(8). Quack, M., Merkt, F., editors. Handbook of High-resolution Spectroscopy. John Wiley & Sons, Inc; 2011. p. 2182

(9). Carter S, Sharma AR, Bowman JM, Rosmus P, Tarroni R. Calculations of Rovibrational Energies and Dipole Transition Intensities for Polyatomic Molecules Using MULTIMODE. J Chem Phys. 2009; 131:224106. [PubMed: 20001023]

(10). Carrington T, Wang X-G. Computing ro-vibrational spectra of van der Waals molecules. WIREs Comput Mol Sci. 2011; 1:952–963.

(11). Tennyson J. Accurate variational calculations for line lists to model the vibration-rotation spectra of hot astrophysical atmospheres. WIREs Comput Mol Sci. 2012; 2:698–715.

(12). Császár AG, Fabri C, Szidarovszky T, Matyus E, Furtenbacher T, Czako G. The Fourth Age of Quantum Chemistry: Molecules in Motion. Phys Chem Chem Phys. 2012; 14:1085–1106. [PubMed: 21997300]

(13). Grimme S. Density Functional Theory with London Dispersion Corrections. WIREs Comput Mol Sci. 2011; 1:211–228.

(14). Goerigk L, Grimme S. Double-hybrid density functionals. WIREs Comput Mol Sci. 2014; 4:576–600.

(15). Burke K, Werschnik J, Gross EKU. Time-dependent density functional theory: Past, present, and future. J Chem Phys. 2005; 123:062206.

(16). Casida ME. Time-dependent density-functional theory for molecules and molecular solids. J Mol Struct Theochem. 2009; 914:3–18.

(17). Cossi M, Barone V. Separation between Fast and Slow Polarizations in Continuum Solvation Models. J Phys Chem A. 2000; 104:10614–10622.

(18). Marenich AV, Cramer CJ, Truhlar DG, Guido CA, Mennucci B, Scalmani G, Frisch MJ. Practical computation of electronic excitation in solution: vertical excitation model. Chem Sci. 2011; 2:2143–2161.

(19). Mennucci B. Polarizable continuum model. WIREs Comput Mol Sci. 2012; 2:386–404.

(20). Barone V, Baiardi A, Biczysko M, Bloino J, Cappelli C, Lipparini F. Implementation and Validation of a Multi-purpose Virtual Spectrometer for Large Systems in Complex Environments. Phys Chem Chem Phys. 2012; 14:12404–12422. [PubMed: 22772710]

(21). Barone V, Baiardi A, Bloino J. New Developments of a Multifrequency Virtual Spectrometer: Stereo-Electronic, Dynamical, and Environmental Effects on Chiroptical Spectra. Chirality. 2014; 26:588–600. [PubMed: 24839096]

(22). Licari D, Baiardi A, Biczysko M, Egidi F, Latouche C, Barone V. Implementation of a Graphical User Interface for the Virtual Multifrequency Spectrometer: The VMS-Draw Tool. J Comput Chem. 2015; 36:321–334. [PubMed: 25408126]

(23). Frisch, MJ., Trucks, GW., Schlegel, HB., Scuseria, GE., Robb, MA., Cheeseman, JR., Scalmani, G., Barone, V., Mennucci, B., Petersson, GA., et al. Gaussian 09 Revision D.01. Gaussian Inc; Wallingford CT: 2009.

(24). Aidas K, Angeli C, Bak KL, Bakken V, Bast R, Boman L, Christiansen O, Cimiraglia R, Coriani S, Dahle P. The Dalton quantum chemistry program system. WIREs Comput Mol Sci. 2014; 4:269–284.

(25). Neese F. The ORCA program system. WIREs Comput Mol Sci. 2012; 2:73–78.

(26). Aquilante F, Pedersen TB, Veryazov V, Lindh R. MOLCAS-a software for multiconfigurational quantum chemistry calculations. WIREs Comput Mol Sci. 2013; 3:143–149.

(27). Barone V, Biczysko M, Bloino J. Fully Anharmonic IR and Raman Spectra of Medium-size Molecular Systems: Accuracy and Interpretation. Phys Chem Chem Phys. 2014; 16:1759–1787. [PubMed: 24346191]

(28). Furche F, Ahlrichs R. Erratum: Time-dependent density functional methods for excited state propertiesİ [J. Chem. Phys. 117, 7433 (2002)]. J Chem Phys. 2004; 121:12772.

(29). Scalmani G, Frisch MJ, Mennucci B, Tomasi J, Cammi R, Barone V. Geometries and properties of excited states in the gas phase and in solution: Theory and application of a time-dependent density functional theory polarizable continuum model. J Chem Phys. 2006; 124:094107.

(30). Liu J, Liang W. Analytical approach for the excited-state Hessian in time-dependent density functional theory: Formalism, implementation, and performance. J Chem Phys. 2011; 135:184111. [PubMed: 22088056]

(31). Liu J, Liang W. Analytical second derivatives of excited-state energy within the time-dependent density functional theory coupled with a conductor-like polarizable continuum model. J Chem Phys. 2013; 138:024101. [PubMed: 23320662]

(32). Bloino J, Biczysko M, Crescenzi O, Barone V. Integrated Computational Approach to Vibrationally Resolved Electronic Spectra: Anisole as a Test Case. J Chem Phys. 2008; 128:244105. [PubMed: 18601315]

(33). Palmer MH, Ridley T, Hoffmann SV, Jones NC, Coreno M, de Simone M, Grazioli C, Biczysko M, Baiardi A. The Ionic States of Iodobenzene Studied by Photoionization and *ab initio* Configuration Interaction and DFT Computations. J Chem Phys. 2015; 142:134301. [PubMed: 25854237]

(34). Barone V, Biczysko M, Borkowska-Panek M, Bloino J. A Multifrequency Virtual Spectrometer for Complex Bio-Organic Systems: Vibronic and Environmental Effects on the UV/Vis Spectrum of Chlorophyll-a. ChemPhysChem. 2014; 15:3355–3364. [PubMed: 25182331]

(35). Neugebauer J, Baerends EJ, Nooijen M, Autschbach J. Importance of vibronic effects on the circular dichroism spectrum of dimethyloxirane. J Chem Phys. 2005; 122:234305. [PubMed: 16008439]

(36). Carta L, Biczysko M, Bloino J, Licari D, Barone V. Environmental and complexation effects on the structures and spectroscopic signatures of organic pigments relevant to cultural heritage: the case of alizarin and alizarin-Mg(ii)/Al(iii) complexes. Phys Chem Chem Phys. 2014:2897–2911. [PubMed: 24424261]

(37). Barone V, Biczysko M, Brancato G. Extending the Range of Computational Spectroscopy by QM/MM Approaches: Time-Dependent and Time-Independent Routes. Adv Quantum Chem. 2010; 59:17.

(38). Lipparini F, Barone V. Polarizable Force Fields and Polarizable Continuum Model: A Fluctuating Charges/PCM Approach. 1. Theory and Implementation. J Chem Theory Comput. 2011; 7:3711–3724. [PubMed: 26598266]

(39). Carnimeo I, Cappelli C, Barone V. Analytical gradients for MP2, double hybrid functionals, and TD-DFT with polarizable embedding described by fluctuating charges. J Comput Chem. 2015; doi: 10.1002/jcc.24195

(40). Brancato G, Barone V, Rega N. Theoretical Modeling of Spectroscopic Properties of Molecules in Solution: Toward an Effective Dynamical Discrete/continuum Approach. Theoret Chim Acta. 2007; 117:1001–1015.

(41). Egidi F, Bloino J, Cappelli C, Barone V. A Robust and Effective Time-Independent Route to the Calculation of Resonance Raman Spectra of Large Molecules in Condensed Phases with the Inclusion of Duschinsky, Herzberg-Teller, Anharmonic, and Environmental Effects. J Chem Theory Comput. 2014; 10:346–363. [PubMed: 26550003]

(42). Born M, Oppenheimer R. Zur Quantentheorie der Molekeln. Annalen der Physik. 1927; 389:457–484.

(43). Biczysko M, Bloino J, Brancato G, Cacelli I, Cappelli C, Ferretti A, Lami A, Monti S, Pedone A, Prampolini G, Puzzarini C, et al. Integrated Computational Approaches for Spectroscopic Studies of Molecular Systems in the Gas Phase and in Solution: Pyrimidine as a Test Case. Theor Chem Acc. 2012; 131:1201/1–19.

(44). Pulay P, Meyer W, Boggs JE. Cubic Force Constants and Equilibrium Geometry of Methane from Hartree–Fock and Correlated Wavefunctions. J Chem Phys. 1978; 68:5077–5085.

(45). Demaison, J.Boggs, JE., Császár, AG., editors. Equilibrium Molecular Structures: From Spectroscopy to Quantum Chemistry. CRC Press, Taylor & Francis Group; 2011.

(46). Raghavachari K, Trucks GW, Pople JA, Head-Gordon M. A Fifth-order Perturbation Comparison of Electron Correlation Theories. Chem Phys Lett. 1989; 157:479–483.

(47). Barone V, Biczysko M, Bloino J, Puzzarini C. The Performance of Composite Schemes and Hybrid CC/DFT Model in Predicting Structure, Thermodynamic and Spectroscopic Parameters: the Challenge of the Conformational Equilibrium in Glycine. Phys Chem Chem Phys. 2013; 15:10094–10111. [PubMed: 23599122]

(48). Piccardo M, Penocchio E, Puzzarini C, Biczysko M, Barone V. Semi-Experimental Equilibrium Structure Determinations by Employing B3LYP/SNSD Anharmonic Force Fields: Validation and Application to Semirigid Organic Molecules. J Phys Chem A. 2015; 119:2058–2082. [PubMed: 25648634]

(49). Penocchio E, Piccardo M, Barone V. Semi-Experimental Equilibrium Structures for Building Blocks of Organic and Biological Molecules: the B2PLYP Route. J Chem Theory Comput. 0; 0doi: 10.1021/acs.jctc.5b00622

(50). Barone V. Anharmonic Vibrational Properties by a Fully Automated Second-order Perturbative Approach. J Chem Phys. 2005; 122:014108.

(51). Puzzarini C, Biczysko M, Barone V. Accurate Harmonic/Anharmonic Vibrational Frequencies for Open-Shell Systems: Performances of the B3LYP/N07D Model for Semirigid Free Radicals Benchmarked by CCSD(T) Computations. J Chem Theory Comput. 2010; 6:828–838. [PubMed: 26613310]

(52). Cheeseman JR, Frisch MJ. Basis Set Dependence of Vibrational Raman and Raman Optical Activity Intensities. J Chem Theory Comput. 2011; 7:3323–3334. [PubMed: 26598166]

(53). Bloino J, Biczysko M, Barone V. General Perturbative Approach for Spectroscopy, Thermodynamics, and Kinetics: Methodological Background and Benchmark Studies. J Chem Theory Comput. 2012; 8:1015–1036. [PubMed: 26593363]

(54). Carnimeo I, Puzzarini C, Tasinato N, Stoppa P, Charmet AP, Biczysko M, Cappelli C, Barone V. Anharmonic Theoretical Simulations of Infrared Spectra of Halogenated Organic Compounds. J Chem Phys. 2013; 139 074310.

(55). Dunning TH. Gaussian Basis Sets for Use in Correlated Molecular Calculations. I. The Atoms Boron through Neon and Hydrogen. J Chem Phys. 1989; 90:1007.

(56). Papajak E, Leverentz HR, Zheng J, Truhlar DG. Efficient Diffuse Basis Sets: cc-pVxZ+ and maug-cc-pVxZ. J Chem Theory Comput. 2009; 5:1197–1202. [PubMed: 26609710]

(57). Biczysko M, Panek P, Scalmani G, Bloino J, Barone V. Harmonic and Anharmonic Vibrational Frequency Calculations with the Double-Hybrid B2PLYP Method: Analytic Second Derivatives and Benchmark Studies. J Chem Theory Comput. 2010; 6:2115–2125. [PubMed: 26615939]

(58). Barone V, Cimino P. Validation of the B3LYP/N07D and PBE0/N07D Computational Models for the Calculation of Electronic g-Tensors. J Chem Theory Comput. 2009; 5:192–199. [PubMed: 26609832]

(59). Barone V, Festa G, Grandi A, Rega N, Sanna N. Accurate Vibrational Spectra of Large Molecules by Density Functional Computations Beyond the Harmonic Approximation: the Case of Uracil and 2-thiouracil. Chem Phys Lett. 2004; 388:279–283.

(60). Zhao Y, Truhlar DG. Density Functionals with Broad Applicability in Chemistry. Acc Chem Research. 2008; 41:157–167. [PubMed: 18186612]

(61). Chai J-D, Head-Gordon M. Systematic optimization of long-range corrected hybrid density functionals. J Chem Phys. 2008; 128:084106/1–15. [PubMed: 18315032]

(62). Fornaro T, Biczysko M, Monti S, Barone V. Dispersion Corrected DFT Approaches for Anharmonic Vibrational Frequency Calculations: Nucleobases and their Dimers. Phys Chem Chem Phys. 2014; 16:10112–10128. [PubMed: 24531740]

(63). Reva IM, Nunes C, Biczysko M, Fausto R. Conformational Switching in Pyruvic Acid Isolated in Ar and N2 Matrixes: Spectroscopic Analysis, Anharmonic Simulation, and Tunneling. J Phys Chem A. 2015; 119:2614–2627. [PubMed: 25332047]

(64). Barone V, Biczysko M, Bloino J, Cimino P, Penocchio E, Puzzarini C. CC/DFT Route toward Accurate Structures and Spectroscopic Features for Observed and Elusive Conformers of Flexible Molecules: Pyruvic Acid as a Case Study. J Chem Theory Comput. 2015; 11:4342–4363. [PubMed: 26575928]

(65). Stephens, PJ., Devlin, FJ., Cheeseman, JR. VCD Spectroscopy for Organic Chemists. CRC Press, Taylor & Francis Group; Boca Raton, FL US: 2012.

(66). Crawford TD, Ruud K. Coupled-Cluster Calculations of Vibrational Raman Optical Activity Spectra. ChemPhysChem. 2011; 12:3442–3448. [PubMed: 21919183]

(67). Gobi S, Magyarfalvi G. Reliability of computed signs and intensities for vibrational circular dichroism spectra. Phys Chem Chem Phys. 2011; 13:16130–16133. [PubMed: 21842039]

(68). Halls MD, Schlegel HB. Comparison study of the prediction of Raman intensities using electronic structure methods. J Chem Phys. 1999; 111:8819–8824.

(69). Dreuw A, Head-Gordon M. Single-Reference ab Initio Methods for the Calculation of Excited States of Large Molecules. Chem Rev. 2005; 105:4009–4037. [PubMed: 16277369]

(70). Jacquemin D, Wathelet V, Perpete EA, Adamo C. Extensive TD-DFT Benchmark: Singlet-Excited States of Organic Molecules. J Chem Theory Comput. 2009; 5:2420–2435. [PubMed: 26616623]

(71). Caricato M, Trucks GW, Frisch MJ, Wiberg KB. Electronic Transition Energies: A Study of the Performance of a Large Range of Single Reference Density Functional and Wave Function Methods on Valence and Rydberg States Compared to Experiment. Journal of Chemical Theory and Computation. 2010; 6:370–383. [PubMed: 26617296]

(72). Isegawa M, Peverati R, Truhlar DG. Performance of recent and high-performance approximate density functionals for time-dependent density functional theory calculations of valence and Rydberg electronic transition energies. J Chem Phys. 2012; 137:244104. [PubMed: 23277925]

(73). Peach MJG, Helgaker T, Salek P, Keal TW, Lutnaes OB, Tozer DJ, Handy NC. Assessment of a Coulomb-attenuated exchange-correlation energy functional. Phys Chem Chem Phys. 2006; 8:558–562. [PubMed: 16482297]

(74). Bloino J, Biczysko M, Santoro F, Barone V. General Approach to Compute Vibrationally Resolved One-Photon Electronic Spectra. J Chem Theory Comput. 2010; 6:1256–1274.

(75). Rauhut G, Hrenar T. A Combined Variational and Perturbational Study on the Vibrational Spectrum of P_2F_4. Chem Phys. 2008; 346:160–166.

(76). Christiansen O. Selected New Developments in Vibrational Structure Theory: Potential Construction and Vibrational Wave Function Calculations. Phys Chem Chem Phys. 2012; 14:6672–6687. [PubMed: 22491444]

(77). Roy TK, Gerber RB. Vibrational Self-Consistent Field Calculations for Spectroscopy of Biological Molecules: New Algorithmic Developments and Applications. Phys Chem Chem Phys. 2013; 15:9468–9492. [PubMed: 23677257]

(78). Nielsen HH. The Vibration-Rotation Energies of Molecules. Reviews of Modern Physics. 1951; 23:90–136.

(79). Mills, IM. Chapter Vibration-Rotation Structure in Asymmetric- and Symmetric-Top Molecules. Molecular Spectroscopy: Modern Research. Rao, KN., Mathews, CW., editors. Academic Press; New York: 1972. p. 115-140.

(80). Barone V. Vibrational Zero-point Energies and Thermodynamic Functions Beyond the Harmonic Approximation. J Chem Phys. 2004; 120:3059–3065. [PubMed: 15268458]

(81). Barone V, Bloino J, Guido CA, Lipparini F. A Fully Automated Implementation of VPT2 Infrared Intensities. Chem Phys Lett. 2010; 496:157–161.

(82). Bloino J, Barone V. A Second-order Perturbation Theory Route to Vibrational Averages and Transition Properties of Molecules: General Formulation and Application to Infrared and

Europe PMC Funders Author Manuscripts

Vibrational Circular Dichroism Spectroscopies. J Chem Phys. 2012; 136:124108. [PubMed: 22462836]

(83). Bloino J. A VPT2 Route to Near-Infrared Spectroscopy: The Role of Mechanical and Electrical Anharmonicity. J Phys Chem A. 2015; 119:5269–5287. [PubMed: 25535769]

(84). Piccardo M, Bloino J, Barone V. Generalized Vibrational Perturbation Theory for Rotovibrational Energies of Linear, Symmetric and Asymmetric Tops: Theory, Approximations and Automated Approaches to Deal with Medium-to-Large Molecular Systems. Int J Quantum Chem. 2015; 115:948–982. [PubMed: 26345131]

(85). Eckart C. Some Studies Concerning Rotating Axes and Polyatomic Molecules. Physical Review. 1935; 47:552–558.

(86). Van Vleck JH. On σ-Type Doubling and Electron Spin in the Spectra of Diatomic Molecules. Physical Review. 1929; 33:467–506.

(87). Krasnoshchekov SV, Isayeva EV, Stepanov NF. Numerical-Analytic Implementation of the Higher-Order Canonical Van Vleck Perturbation Theory for the Interpretation of Medium-Sized Molecule Vibrational Spectra. J Phys Chem A. 2012; 116:3691–3709. [PubMed: 22369280]

(88). Rosnik AM, Polik WF. VPT2+K Spectroscopic Constants and Matrix Elements of the Transformed Vibrational Hamiltonian of a Polyatomic Molecule with Resonances using Van Vleck Perturbation Theory. Mol Phys. 2014; 112:261–300.

(89). Montero S. Anharmonic Raman intensities of overtones, combination and difference bands. J Chem Phys. 1982; 77:23–29.

(90). Bouř P. Anharmonic Corrections to Vibrational Energies of Molecules: Water and Dideuteriooxirane. J Phys Chem. 1994; 98:8862–8865.

(91). Faulkner TR, Marcott C, Moscowitz A, Overend J. Anharmonic effects in vibrational circular dichroism. J Am Chem Soc. 1977; 99:8160–8168.

(92). Willets A, Handy NC, Green WH Jr, Jayatilaka D. Anharmonic Corrections to Vibrational Transition Intensities. Journal of Physical Chemistry. 1990; 94:5608–5616.

(93). Vázquez J, Stanton JF. Simple(r) Algebraic Equation for Transition Moments of Fundamental Transitions in Vibrational Second-order Perturbation Theory. Mol Phys. 2006; 104:377–388.

(94). Vázquez J, Stanton JF. Treatment of Fermi Resonance Effects on Transition Moments in Vibrational Perturbation Theory. Mol Phys. 2007; 105:101–109.

(95). Martin JML, Lee TJ, Taylor PM, François J-P. The Anharmonic Force Field of Ethylene, C_2H_4, by Means of Accurate ab initio Calculations. J Chem Phys. 1995; 103:2589–2602.

(96). Krasnoshchekov SV, Isayeva EV, Stepanov NF. Criteria for First- and Second-order Vibrational Resonances and Correct Evaluation of the Darling-Dennison Resonance Coefficients Using the Canonical Van Vleck Perturbation Theory. J Chem Phys. 2014; 141:234114. [PubMed: 25527926]

(97). Kuhler KM, Truhlar DG, Isaacson AD. General method for removing resonance singularities in quantum mechanical perturbation theory. J Chem Phys. 1996; 104:4664–4670.

(98). Martin JML, Taylor PM. Accurate ab initio quartic force field for trans-HNNH and treatment of resonance polyads. Spectrochimica Acta Part A: Molecular Spectroscopy. 1997; 53:1039–1050.

(99). Gaw JF, Yamaguchi Y, Schaefer HF, Handy NC. Generalization of analytic energy third derivatives for the RHF closed-shell wave function: Derivative energy and integral formalisms and the prediction of vibrationŰrotation interaction constants. J Chem Phys. 1986; 85:5132–5142.

(100). Colwell SM, Jayatilaka D, Maslen PE, Amos RD, Handy NC. Higher analytic derivatives. I. A new implementation for the third derivative of the SCF energy. Int J Quantum Chem. 1991; 40:179–199.

(101). Maslen PE, Jayatilaka D, Colwell SM, Amos RD, Handy NC. Higher analytic derivatives. II. The fourth derivative of self-consistent-field energy. J Chem Phys. 1991; 95:7409–7417.

(102). Ringholm M, Jonsson D, Bast R, Gao B, Thorvaldsen AJ, Ekström U, Helgaker T, Ruud K. Analytic cubic and quartic force fields using density-functional theory. J Chem Phys. 2014; 140:034103. [PubMed: 25669359]

(103). Merten C, Bloino J, Barone V, Xu Y. Anharmonicity Effects in the Vibrational CD Spectra of Propylene Oxide. J Phys Chem Lett. 2013; 4:3424–3428.

Europe PMC Funders Author Manuscripts

(104). Barone V, Biczysko M, Bloino J, Puzzarini C. Accurate Molecular Structures and Infrared Spectra of trans-2,3-dideuterooxirane, Methyloxirane, and trans-2,3-dimethyloxirane. J Chem Phys. 2014; 141:034107/1–17. [PubMed: 25053301]

(105). Covington CL, Polavarapu PL. Similarity in Dissymmetry Factor Spectra: A Quantitative Measure of Comparison between Experimental and Predicted Vibrational Circular Dichroism. J Phys Chem A. 2013; 117:3377–3386. [PubMed: 23534955]

(106). Tommasini M, Longhi G, Mazzeo G, Abbate S, Nieto-Ortega B, Ramírez FJ, Casado J, Navarrete JTL. Mode Robustness in Raman Optical Activity. J Chem Theory Comput. 2014; 10:5520–5527. [PubMed: 26583235]

(107). Baiardi A, Bloino J, Barone V. General Time Dependent Approach to Vibronic Spectroscopy Including Franck–Condon, Herzberg–Teller, and Duschinsky Effects. J Chem Theory Comput. 2013; 9:4097–4115. [PubMed: 26592403]

(108). Franck J. Elementary processes of photochemical reactions. Transactions of the Faraday Society. 1926; 21:536–542.

(109). Condon EU. Nuclear motions associated with electron transitions in diatomic molecules. Physical Review. 1928; 32:858–872.

(110). Herzberg G, Teller E. Schwingungsstruktur der Elektronenübergänge bei mehratomigen Molekülen. Zeitschrift für Physikalische Chemie - Abteilung B. 1933; 21:410–446.

(111). Duschinsky F. Acta Physicochimica URSS. 1937; 7:551.

(112). Barone V, Bloino J, Biczysko M, Santoro F. Fully Integrated Approach to Compute Vibrationally Resolved Optical Spectra: From Small Molecules to Macrosystems. J Chem Theory Comput. 2009; 5:540–554. [PubMed: 26610221]

(113). Santoro F, Improta R, Lami A, Bloino J, Barone V. Effective method to compute Franck-Condon integrals for optical spectra of large molecules in solution. J Chem Phys. 2007; 126:084509. [PubMed: 17343460]

(114). Santoro F, Lami A, Improta R, Barone V. Effective method to compute vibrationally resolved optical spectra of large molecules at finite temperature in gas phase and in solution. Journal of Chemical Physics. 2007; 126:184102. [PubMed: 17508787]

(115). Tang J, Lee MT, Lin SH. Effects of the Duschinsky mode-mixing mechanism on temperature dependence of electron transfer processes. J Chem Phys. 2003; 119

(116). Ianconescu R, Pollak E. Photoinduced Cooling of Polyatomic Molecules in an Electronically Excited State in the Presence of Dushinskii Rotations. J Phys Chem A. 2004; 108:7778–7784.

(117). Baiardi A, Bloino J, Barone V. A General Time-dependent Route to Resonance-Raman Spectroscopy Including Franck-Condon, Herzberg-Teller and Duschinsky Effects. J Chem Phys. 2014; 141:114108. [PubMed: 25240346]

(118). Baiardi A, Latouche C, Bloino J, Barone V. Accurate yet feasible computations of resonance Raman spectra for metal complexes in solution: $[Ru(bpy)_3]^{2+}$ as a case study. Dalton Trans. 2014; 43:17610–17614. [PubMed: 25207752]

(119). Vidal LN, Egidi F, Barone V, Cappelli C. Origin invariance in vibrational resonance Raman optical activity. J Chem Phys. 2015; 142:174101. [PubMed: 25956084]

(120). Neugebauer J, Baerends EJ, Nooijen M, Autschbach J. Importance of vibronic effects on the circular dichroism spectrum of dimethyloxirane. J Chem Phys. 2005; 122:234305. [PubMed: 16008439]

(121). Barone V, Biczysko M, Bloino J, Borkowska-Panek M, Carnimeo I, Panek P. Toward Anharmonic Computations of Vibrational Spectra for Large Molecular Systems. Int J Quantum Chem. 2012; 112:2185–2200.

(122). Kvapilova H, Vlcek A, Barone V, Biczysko M, Zalis S. Anharmonicity Effects in IR Spectra of [Re(X)(CO)3(α-diimine)] (α-diimine=2,2'-bipyridine or pyridylimidazo[1,5-a]pyridine; X=Cl or NCS) Complexes in Ground- and Excited Electronic States. J Phys Chem A. 2015; 119doi: 10.1021/acs.jpca.5b07585

(123). Carnimeo I, Biczysko M, Bloino J, Barone V. Reliable Structural, Thermodynamic, and Spectroscopic Properties of Organic Molecules Adsorbed on Silicon Surfaces from Computational Modeling: the Case of Glycine@Si(100). Phys Chem Chem Phys. 2011; 13:16713–16727. [PubMed: 21858336]

(124). Baiardi A, Bloino J, Barone V. Accurate Simulation of Resonance-Raman Spectra of Flexible Molecules: An Internal Coordinates Approach. J Chem Theory Comput. 2015; 11:3267–3280. [PubMed: 26575763]

(125). Baker J, Kessi A, Delley B. The generation and use of delocalized internal coordinates in geometry optimization. J Chem Phys. 1996; 105:192–212.

(126). Swart M, Matthias Bickelhaupt F. Optimization of strong and weak coordinates. Int J Quantum Chem. 2006; 106:2536–2544.

(127). Fogarasi G, Zhou X, Taylor PW, Pulay P. The calculation of ab initio molecular geometries: efficient optimization by natural internal coordinates and empirical correction by offset forces. J Am Chem Soc. 1992; 114:8191–8201.

(128). Barone V, Polimeno A. Toward an integrated computational approach to CW-ESR spectra of free radicals. Phys Chem Chem Phys. 2006; 8:4609–4629. [PubMed: 17047758]

(129). Tanimura Y. Stochastic Lionville, Langevin, Fokker-Planck, and master equation approaches to quantum dissipative systems. J Phys Soc Jpn. 2006; 75

(130). Zerbetto M, Licari D, Barone V, Polimeno A. Computational tools for the interpretation of electron spin resonance spectra in solution. Mol Phys. 2013; 111:2746–2756.

(131). Sebestik J, Bouř P. Raman Optical Activity of Methyloxirane Gas and Liquid. J Chem Lett. 2011; 2:498–502.

Europe PMC Funders Author Manuscripts

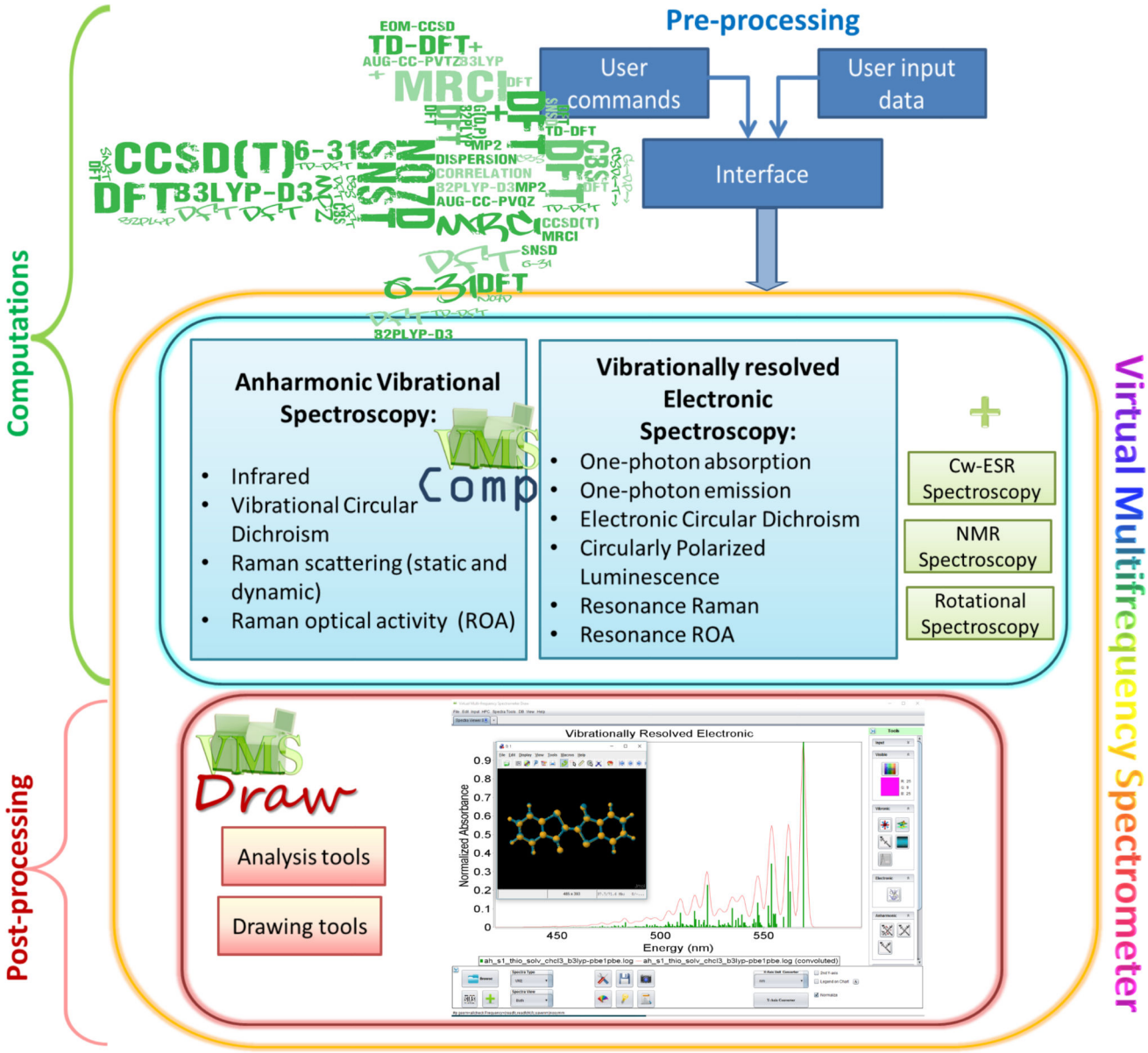

Figure 1.
The framework of the whole VMS project.

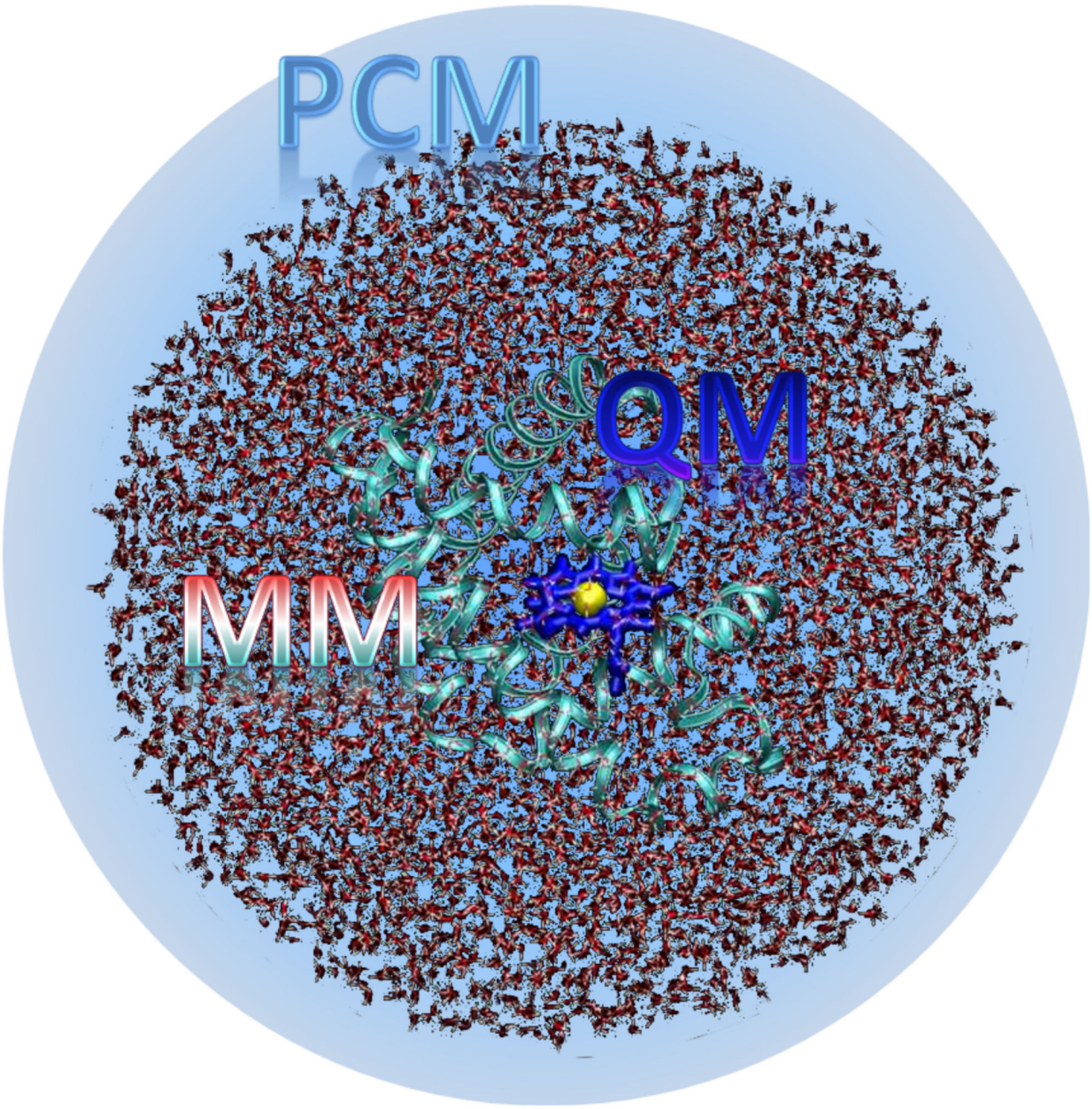

Figure 2.
Fully polarisable multiscale model: QM/MM(FQ)/PCM.

Europe PMC Funders Author Manuscripts

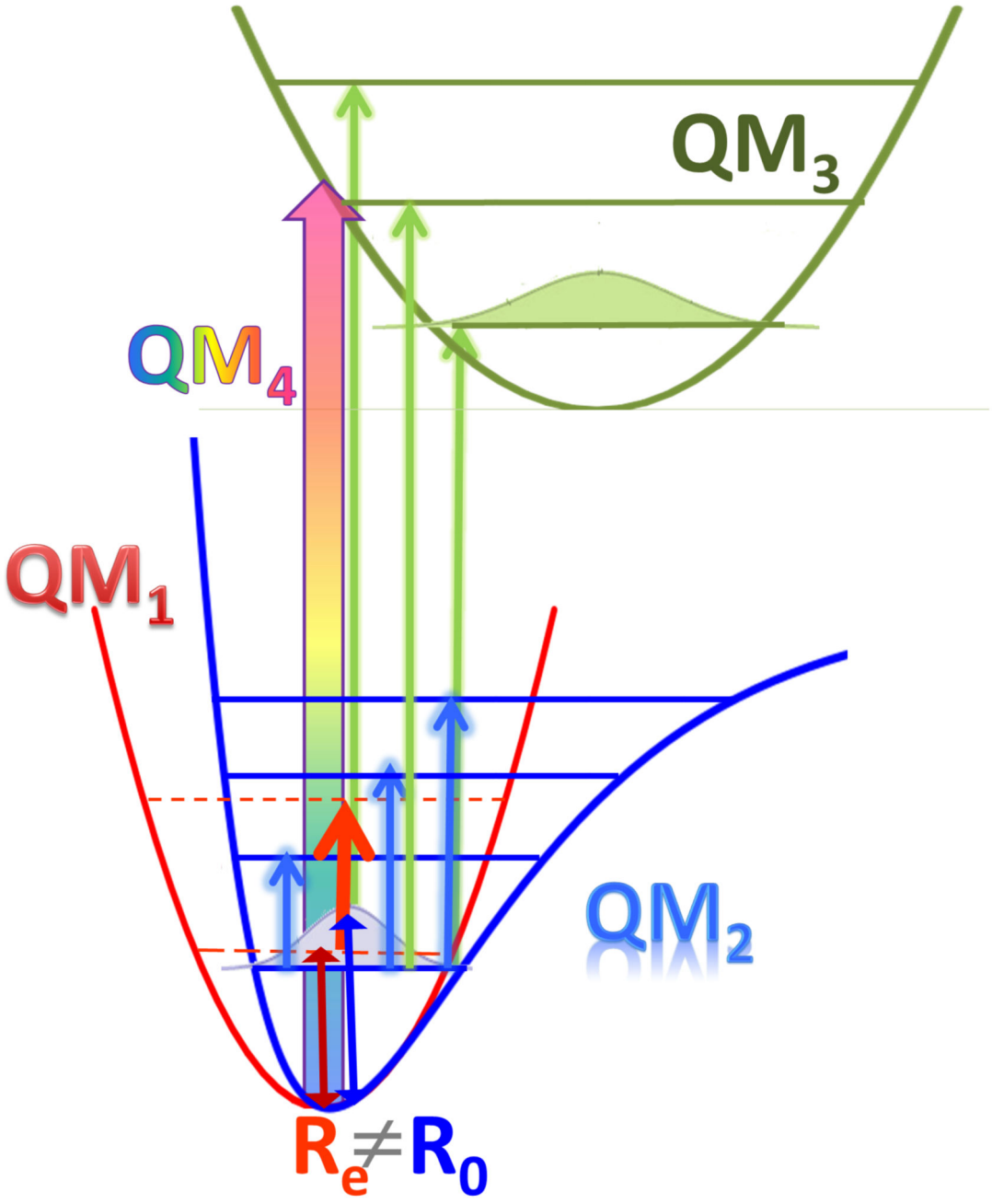

Figure 3.
General theoretical framework for vibrationally averaged properties, together with vibrational and vibronic transitions along with QM models for PES and PS computations.

Europe PMC Funders Author Manuscripts

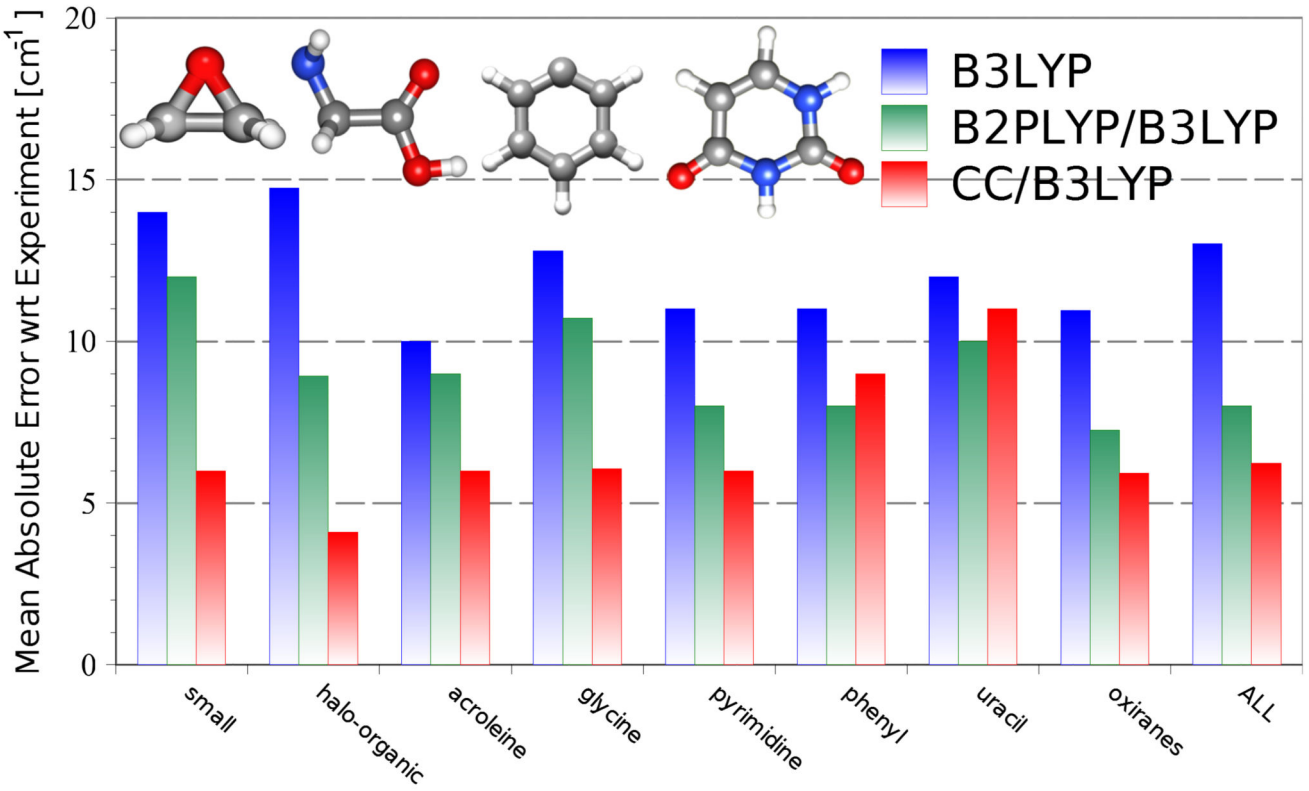

Figure 4.

Performance of B3LYP/SNSD and hybrid B2PLYP/B3LYP and CCSD(T)/B3LYP models for the computation of anharmonic vibrational wavenumbers at the GVPT2 level. All anharmonic corrections have been computed at the B3LYP level with basis sets of at least double-ζ plus polarization quality (mainly belonging to the SNSD/N07D family).i Harmonic wavenumbers at the B2PLYP and CCSD(T) levels have been computed with basis sets of at least cc-pVTZ quality. Mean Absolute Error with respect to experimental data for about 300 fundamental wavenumbers of small-to-medium size molecular systems; Ref.:27 small molecules (H_2O, NH_2, NH_3), halo-organic systems (halo-methanes, halo-ethylenes), acroleine, glycine (Ip, IIn, IIIp and VIp conformers), phenyl, pyrimidine, uracil; Ref.:104 oxiranes (oxirane, trans-2,3-dideuteriooxirane and methyloxirane).

Europe PMC Funders Author Manuscripts

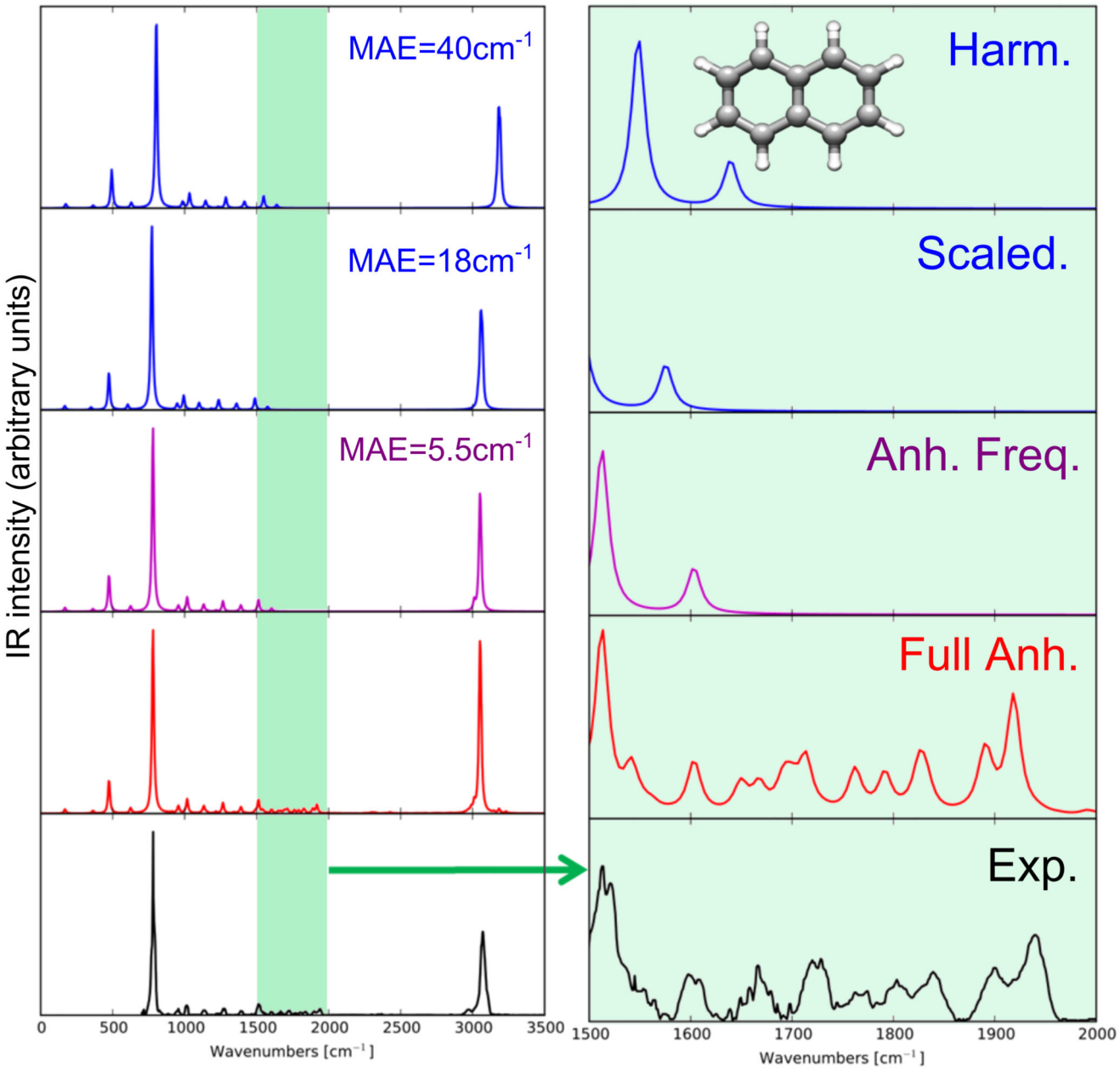

Figure 5.

Theoretical and experimental IR spectra of napthalene in the 300–3600 cm^{-1} range. Fully harmonic (Harm., harmonic wavenumbers and intensities) spectra, scaled harmonic spectra (Scaled., scaled harmonic energies), spectra obtained by combining anharmonic wavenumbers with harmonic intensities (Anh. Freq.) and fully anharmonic spectra (Full Anh., anharmonic wavenumbers and intensities). All computations at the B3LYP/SNSD level, mean absolute error (MAE) with respect to the experiment, see Ref.83 for details.

Europe PMC Funders Author Manuscripts

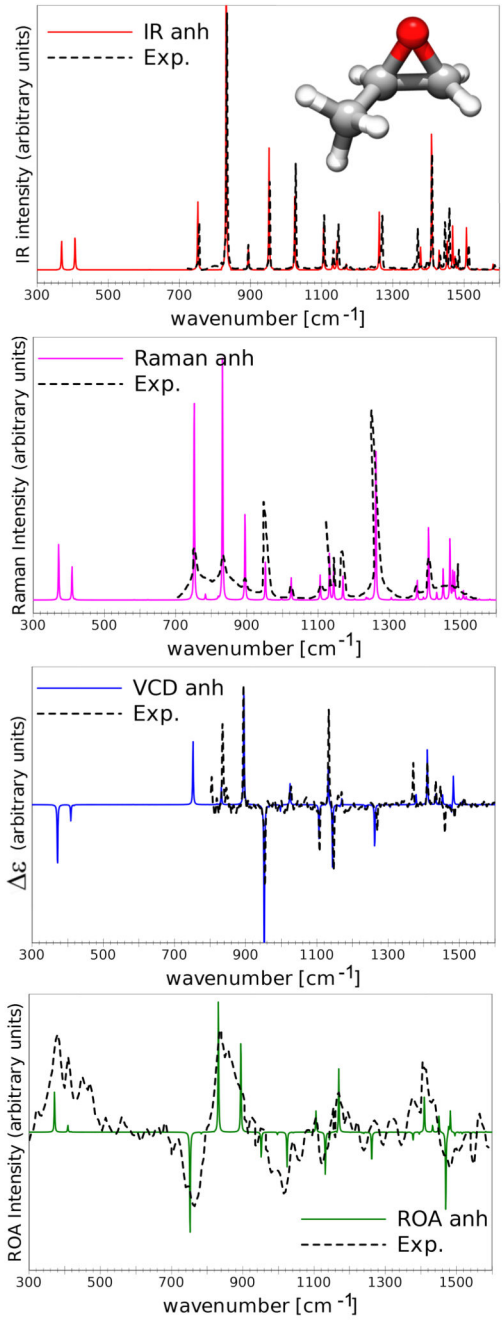

Figure 6.

Fully anharmonic IR, Raman, VCD and ROA spectra of methyloxirane compared to their experimental counterparts measured in low-temperature Ar Matrix (IR, VCD103) or the gas phase (Raman, ROA131). Vibrational wavenumbers have been computed at the ”cheapCC”/B3LYP level104 in conjunction with B3LYP/SNSD intensities; all spectra have been convoluted by means of Lorentzian distribution functions with FWHM 2 cm^{-1}.

Europe PMC Funders Author Manuscripts

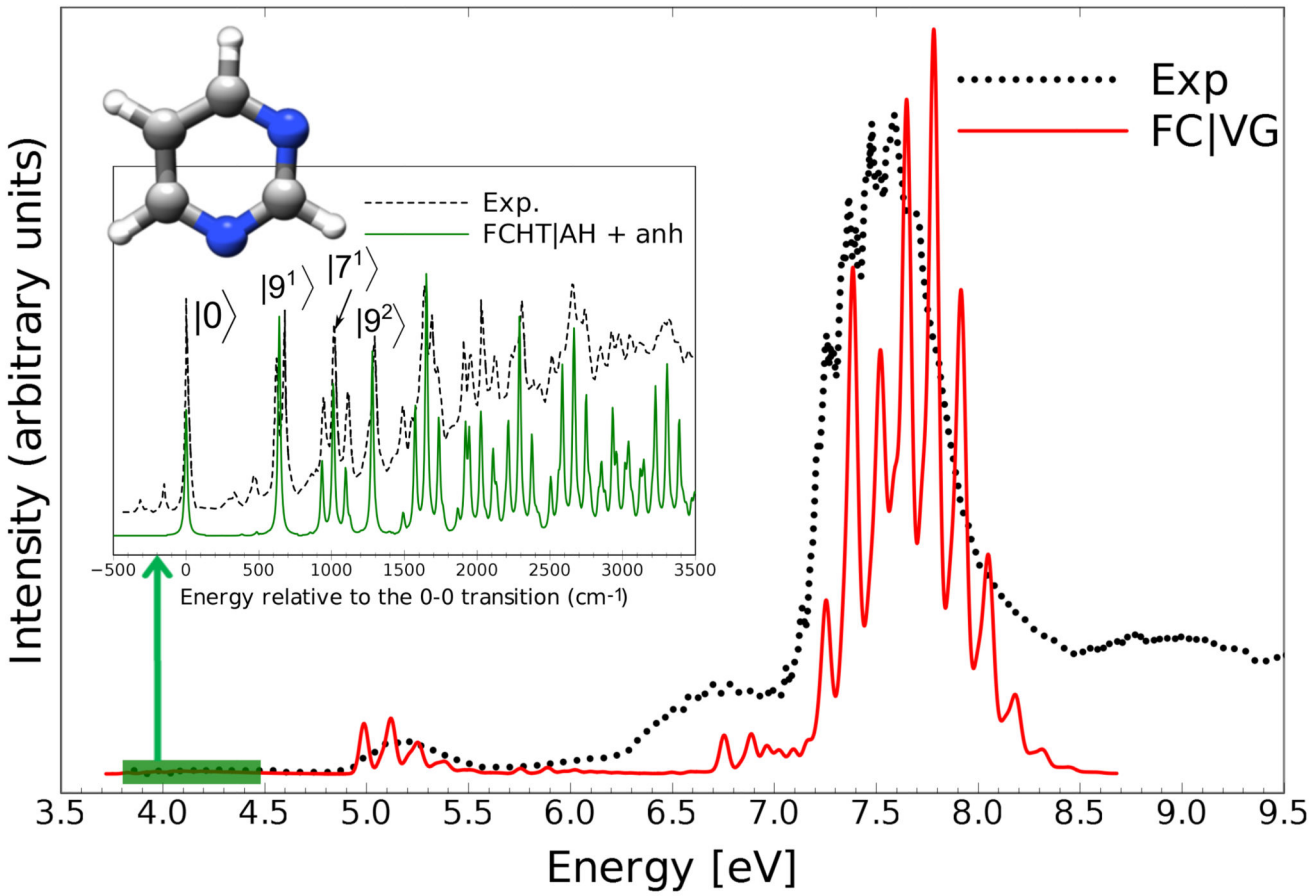

Figure 7.

Theoretical and experimental spectra of isolated pyrimidine in the 3.5-9.5 eV energy range computed at the FC/VG level, applying the hybrid pHF/DFT approach (main panel, red). The $S_1 \leftarrow S_0$ electronic transition along with the assignment of the most intense vibronic bands, computed at the FCHT/AH level, with anharmonic corrections though effective scaling procedure using the best CC/B3LYP estimates for the electronic ground-state (inset, green). See Ref.43 for details.

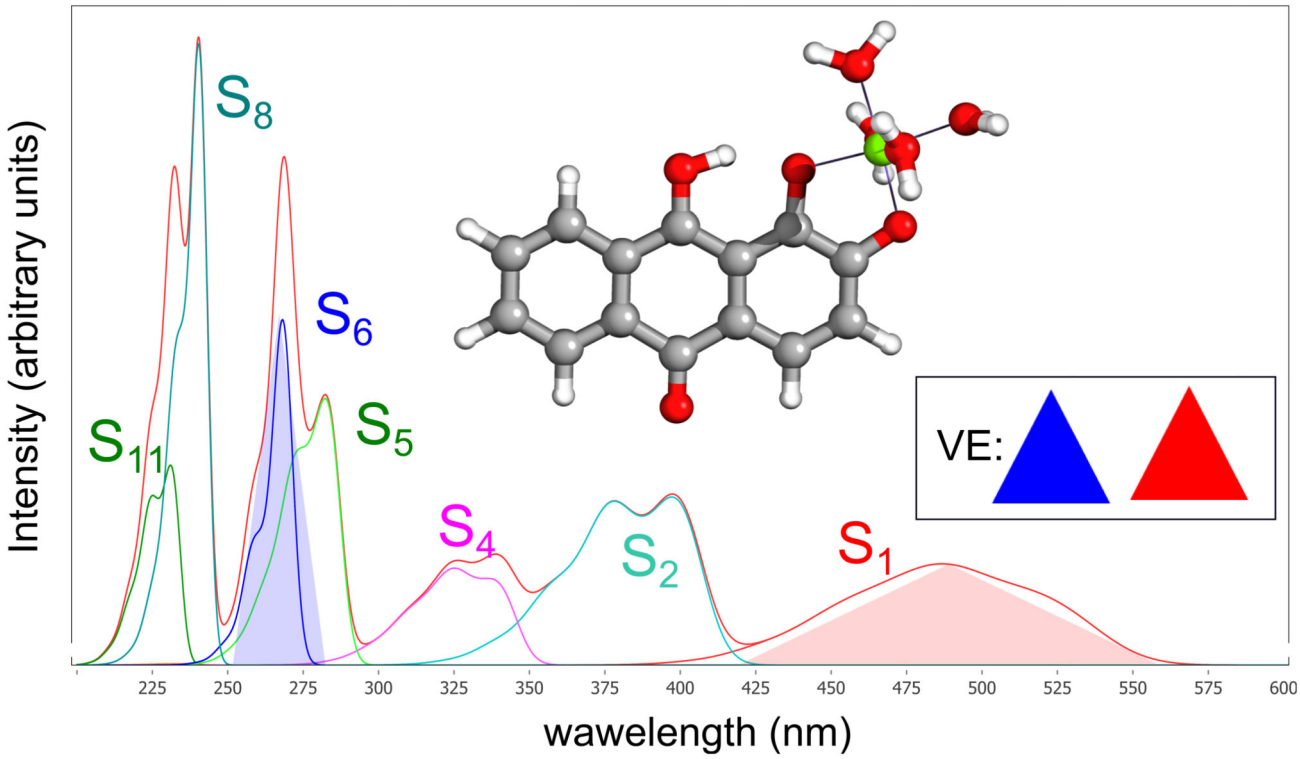

Figure 8.

Total simulated VG/FC spectrum of the 1,2Al-PT9(H_2O)$_4$ alizarin complex, along with the single-state contributions to the spectra band shape. See Ref.36 for details.

Europe PMC Funders Author Manuscripts

Europe PMC Funders Author Manuscripts

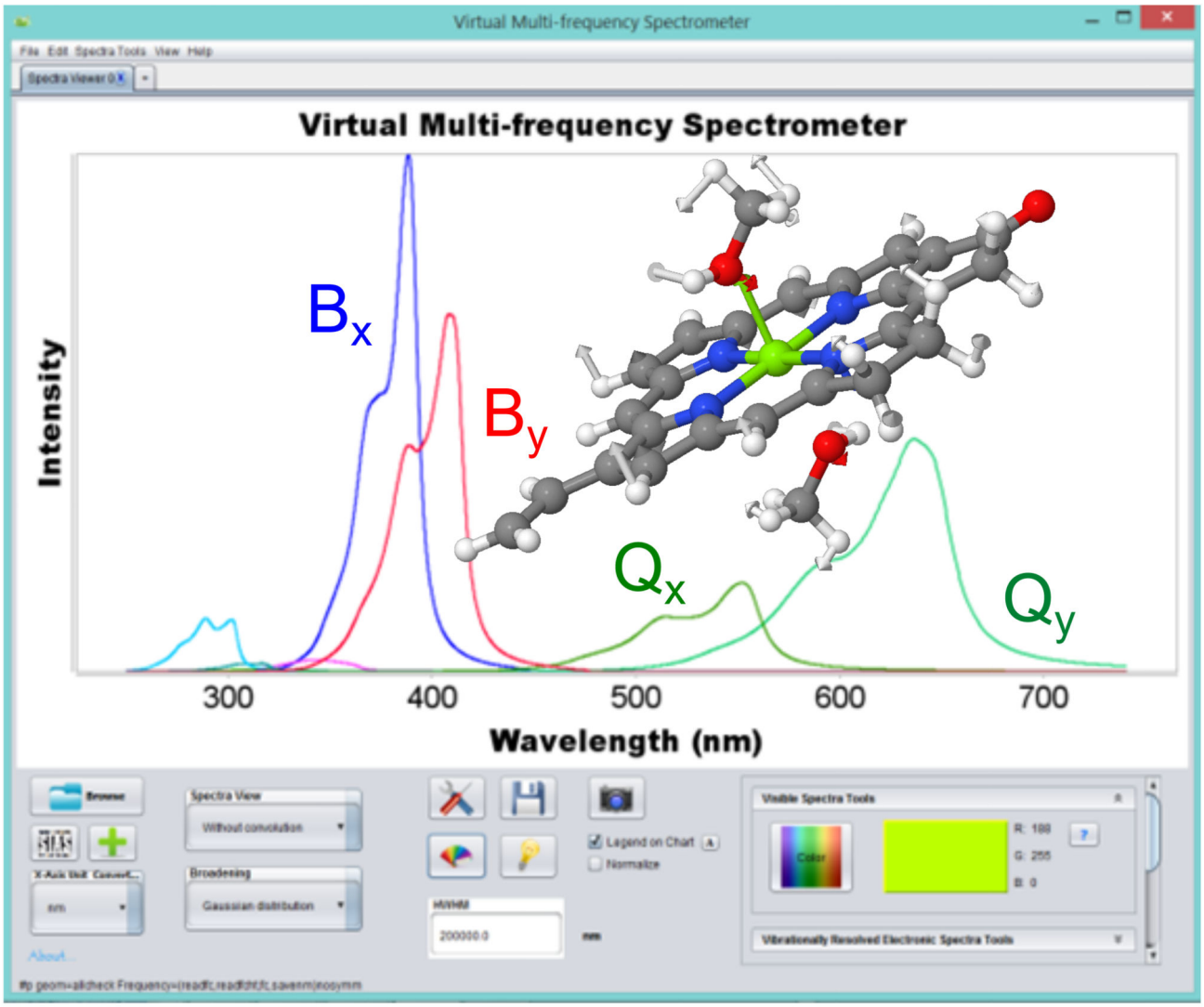

Figure 9.

Simulated UV-vis spectrum of chlorophyll-*a* analyzed by VMS-draw: total spectrum obtained as the sum of separate electronic transitions, predicted colour as perceived by a human eye, and normal mode visualisation.

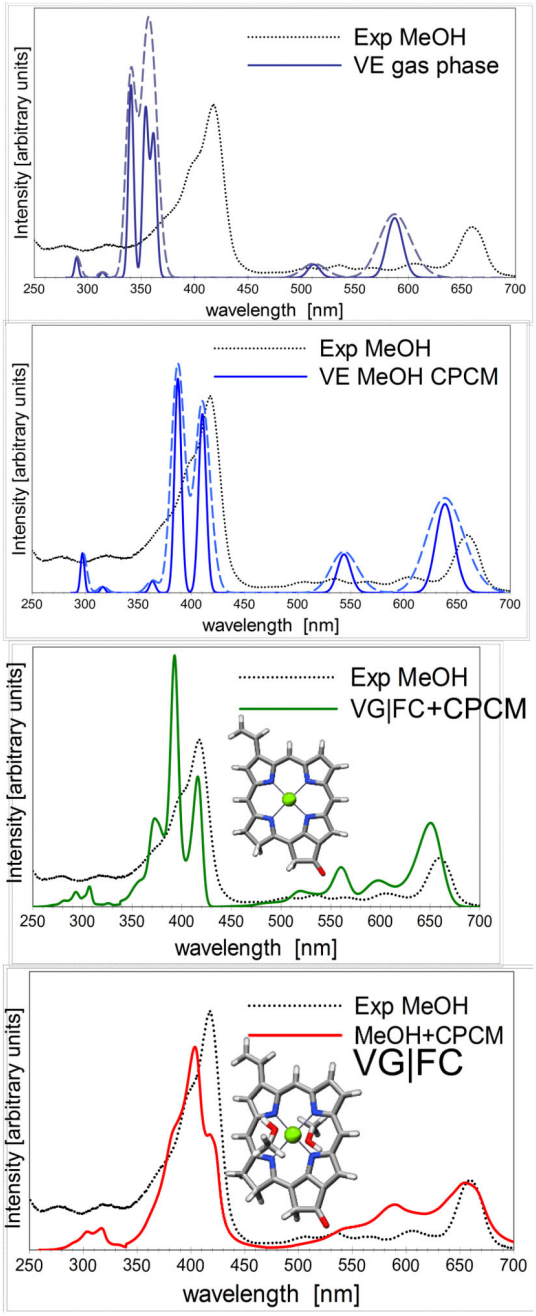

Figure 10.

Contributions of various effects (bulk solvent (CPCM), vibronic contributions (FC/VG) of intramolecular vibrations, and 2 explicit methanol molecules) to the overall absorbtion spectrum of chlorophyll *a1* in the 250-700 nm energy range, as compared to the experimental data obtained in methanol solution, see Ref. 34 for details.

Europe PMC Funders Author Manuscripts

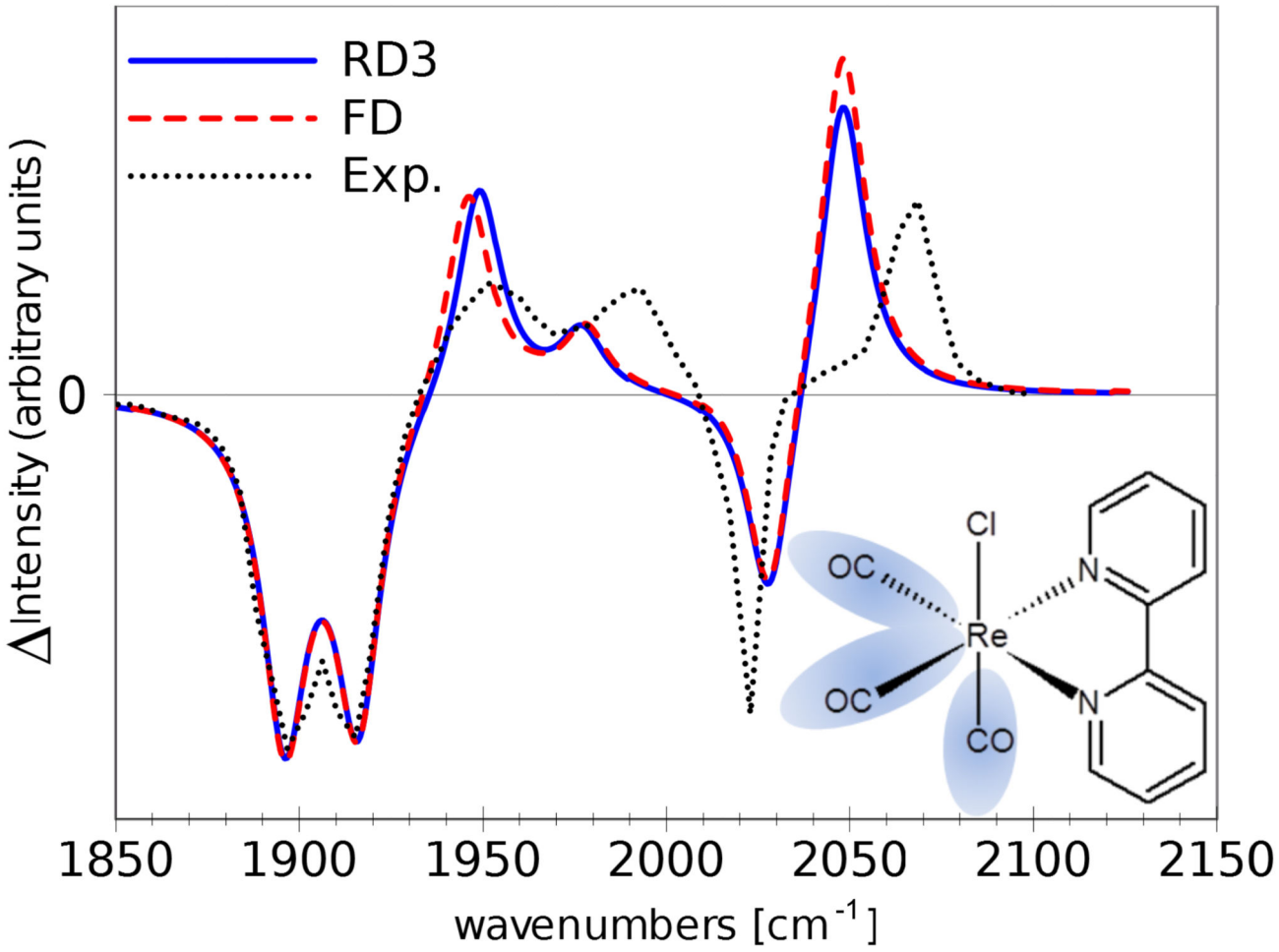

Figure 11.

Experimental and theoretical anharmonic difference TRIR spectra of Rebpy. Anharmonic spectra have been calculated using the three-mode reduced (RD3) and full (FD) dimensionality approaches.

Europe PMC Funders Author Manuscripts

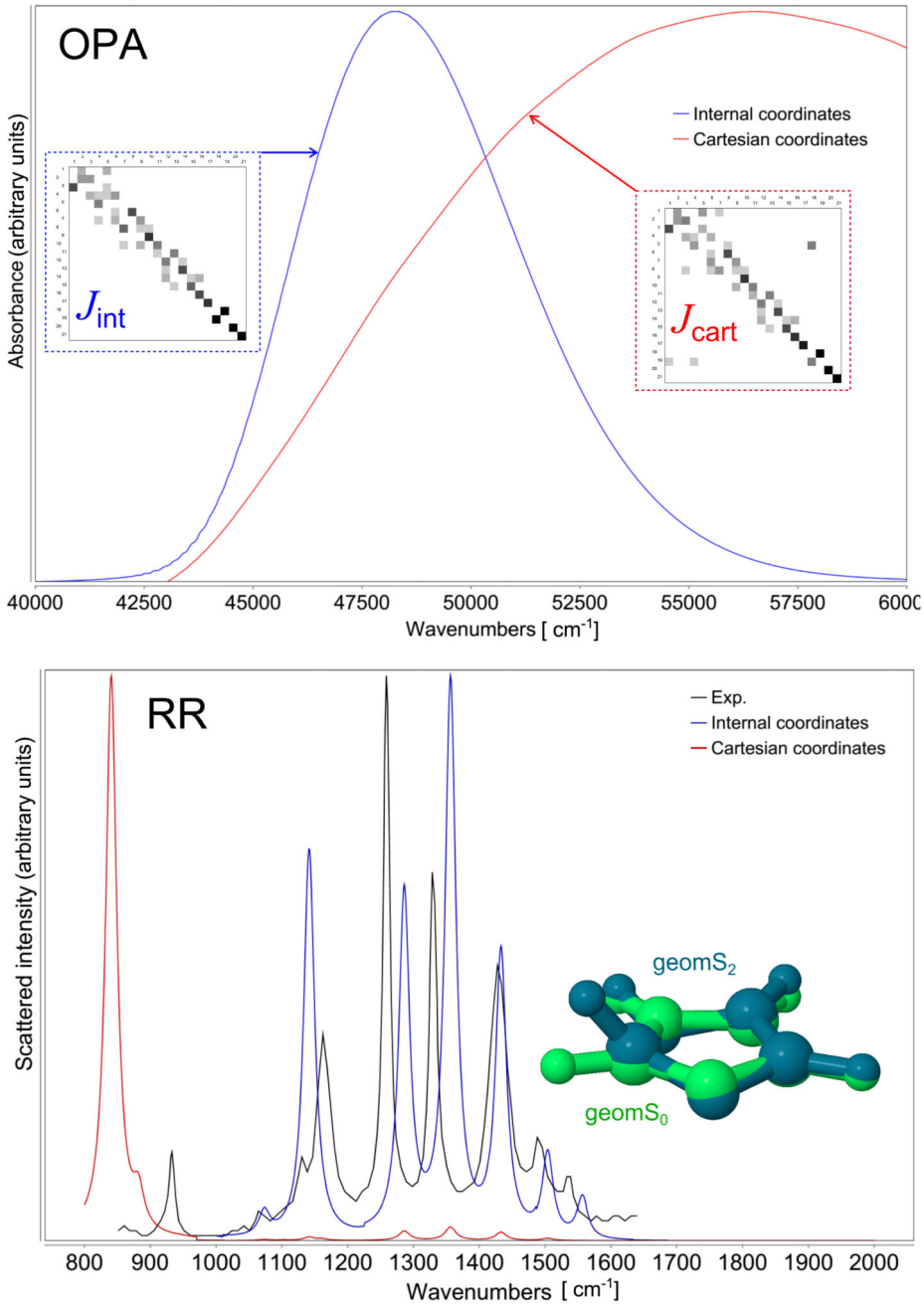

Figure 12.

Theoretical OPA (upper panel) and RR (lower panel) spectra for the $S_2 \leftarrow S_0$ transition of imidazole in water. All simulations have been carried out using the TD AH/FC algorithm with normal modes built with cartesian or internal coordinates. Electronic structure calculations have been carried out at the DFT (S_0) and TD-DFT (S_2) level including bulk solvent contributions by means of the PCM. Broadening effects have been included using Gaussian functions with HWHM of 100 cm^{-1} (for the OPA spectrum) and Lorenztian functions with HWHM of 10 cm^{-1} (for the RR spectrum). The equilibrium geometriesy of

both electronic states are also shown, along with the The Duschinsky matrices (**J**) computed using cartesian or internal coordinates. The elements of J_{ij}^2 are calculated and a shade of gray is associated with each element (i,j) in the figure based on its absolute value (0, white; 1, black).

Europe PMC Funders Author Manuscripts

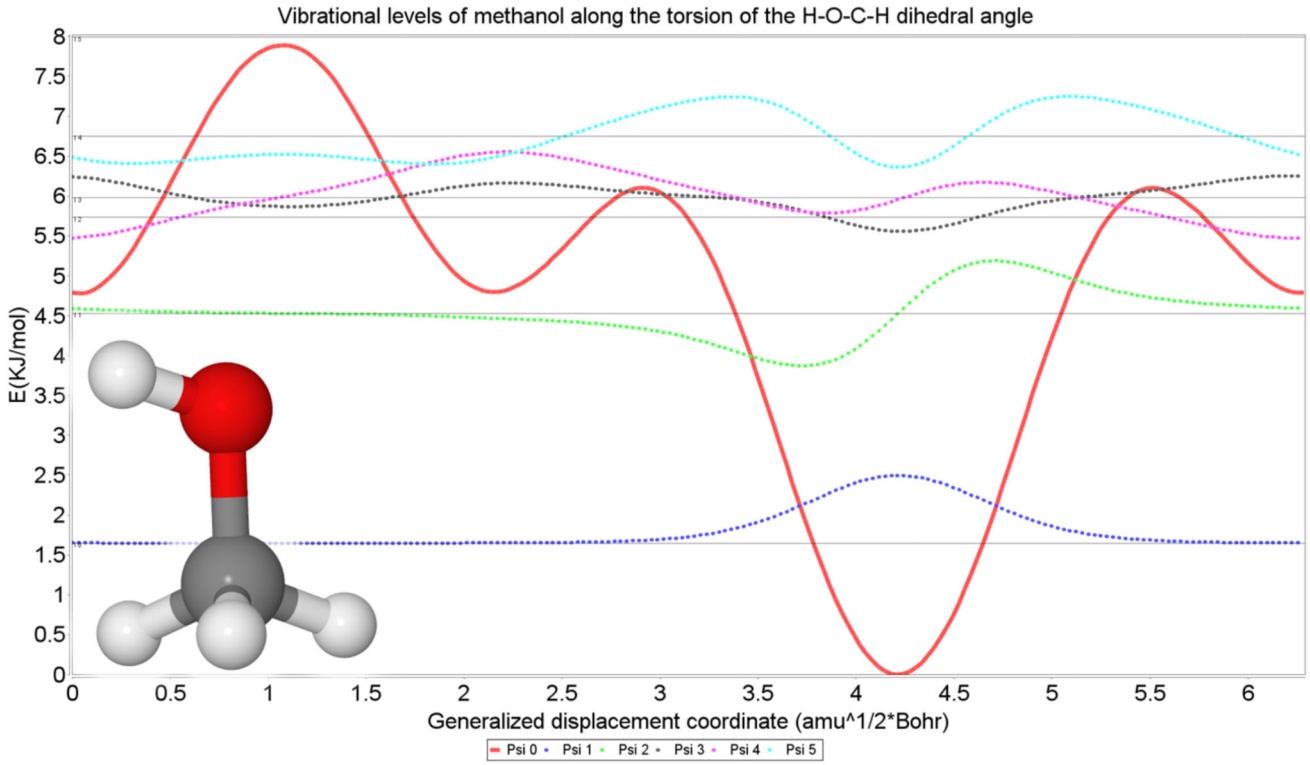

Figure 13.

Vibrational(torsional) energy levels and one-dimensional vibrational wavefunctions of methanol superimposed to the potential energy profile along the HOCH dihedral angle.

Europe PMC Funders Author Manuscripts

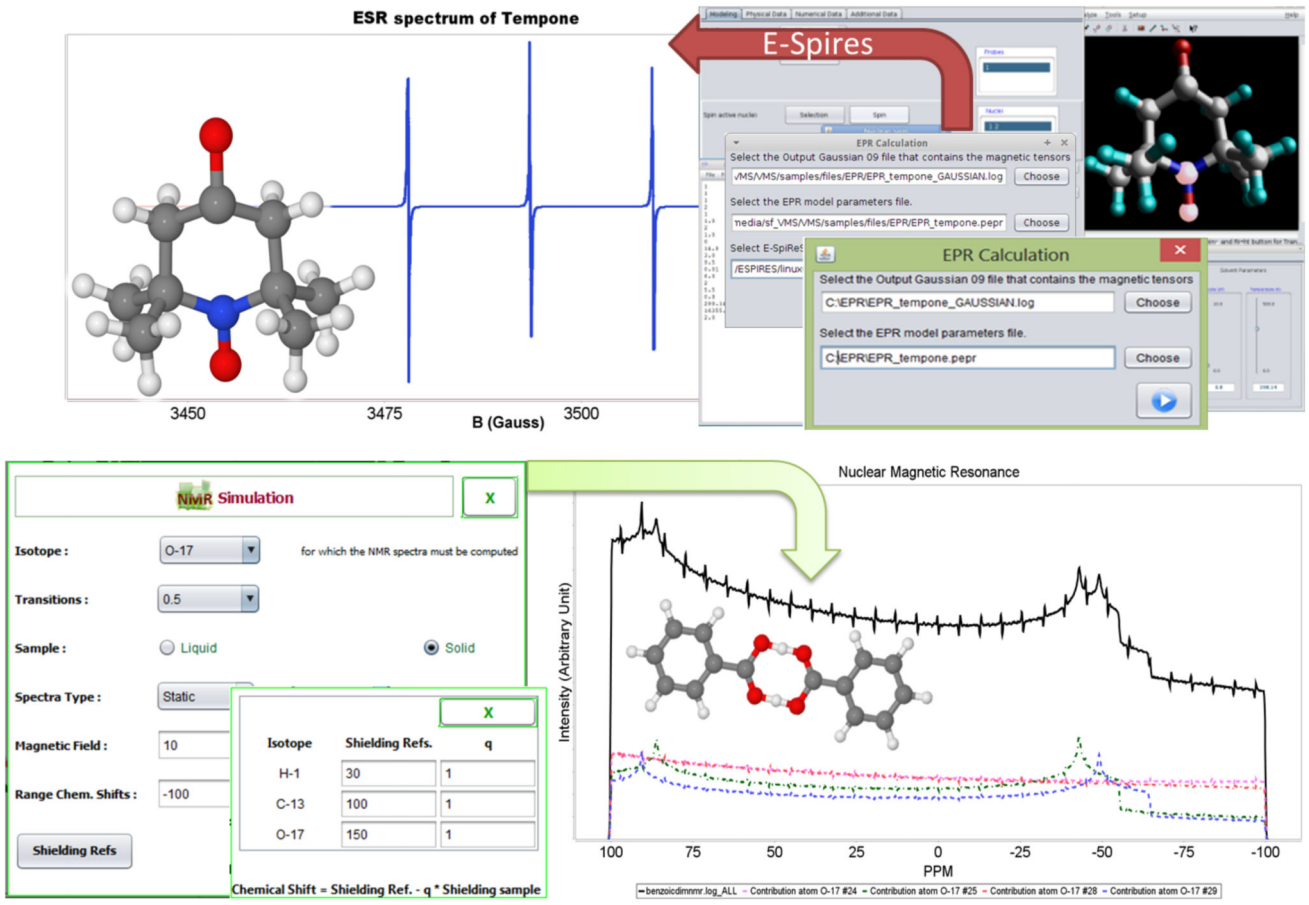

Figure 14.

EPR spectrum of tempone (upper panel) and NMR spectrum of benzoic acid dimer (lower panel).In the latter case, the total spectrum is plotted in black and the contributions of different ^{17}O in various colours.

Europe PMC Funders Author Manuscripts

Europe PMC Funders Author Manuscripts

Table 1

Accuracy of different QM and QM/QM' models: fundamental and non-fundamental transitions of pyruvic acid[a].

harm QM	anh QM'	fundamentals[b]		ALL[c]	
		MAE	**|MAX|**	**MAE**	**|MAX|**
B3LYP[d]		15	46	28	71
B2PLYP[e]		8	36	17	54
CCSD(T)[f]	B3LYP[d]	6	27	8	34
CCSD(T)[f]	B2PLYP[e]	5	24	7	25[g]

[a] Theoretical results are compared with experimental data for all fundamental and over 50 non-fundamental transitions up to 7000 cm^{-1}.64

[b] Mean absolute error (MAE) and maximum absolute deviations (|MAX|) with respect to experiment evaluated for fundamental transitions.

[c] Mean absolute error (MAE) and maximum absolute deviations (/MAX/) with respect to experiment evaluated for all reported bands.

[d] in conjunction with the SNSD basis set, this work.

[e] in conjunction with the aug-cc-pVTZ basis set, see.64

[f] best theoretical estimates from composite scheme, see.64

[g] Except 2 νOH for Tc conformer (discrepancy of 41 cm^{-1})

Europe PMC Funders Author Manuscripts

Table 2

Experimental and calculated vibrational wavenumbers (cm^{-1}) of the three C=O stretching modes of **Rebpy**[a].

Electronic State	Mode ν(CO)[b]	Harm.	1M	3M	RD3	FD	Exp.
Ground state	υ9 (A')	2057	2052	2038	2028	2028	2022
	υ10 (A")	1942	1956	1922	1916	1916	1915
	υ11(A')	1921	1922	1902	1896	1896	1896
Lowest triplet state	υ9 (A')	2090	2081	2065	2048	2048	2068
	υ10 (A')	2016	2027	1993	1977	1978	1993
	υ11 (A")	1978	1988	1956	1949	1946	1951

[a] All computations at the B3LYP/6-31+G(d)/Re-(8s7p6d2f1g)/[6s5p3d2f1g]PP/PCM(CH_2Cl_2) level, see Ref.122 for details.

[b] Symmetry labels of approximate C_S symmetry in parenthesis.